

Single-band model of substitutional disordered ternary alloys in the coherent-potential approximation

Leonard M. Scarfone* and James D. Chlipala†

Department of Physics, University of Vermont, Burlington, Vermont 05401

(Received 24 September 1974)

The single-band model Hamiltonian used by Velický, Kirkpatrick, and Ehrenreich (VKE) in their classic paper on the electronic theory of nondilute binary alloys is extended to the ternary-alloy case, and a number of results are derived. It is shown by direct calculation that the coherent-potential approximation (CPA) preserves the first seven moments of the density of states and the spectral density. Diagrammatic considerations put the highest moments at eight and seven, respectively. Exact information concerning the effective Hamiltonian leads via the Kramers-Kronig dispersion relation to a series of sum rules involving the self-energy. The localization theorem predicts the existence of two or three well-separated subbands for which the self-energy may have a pole between adjacent subbands. These singularities are also found in the CPA. Within the appropriate limits, all calculated quantities and various limiting behaviors (virtual crystal, dilute alloy, and the atomic limit), reduce to the binary-alloy results of VKE. A semielliptic reference density of states is used for a numerical presentation of the CPA description of the model ternary alloy. New numerical examples of the \vec{k} -independent properties of the CPA are exhibited for the self-energy, the total density of states, and the partial densities of states, over a wide range of concentrations and scattering-potential strengths. Results are also displayed for the Bloch-wave spectral density. This \vec{k} -dependent quantity provides information concerning the validity of describing the states of the disordered alloy in terms of quasiparticles with wave vector \vec{k} .

I. INTRODUCTION

The problem of understanding the single-particle properties of elementary excitations (electrons, phonons, excitons, magnons) in substitutional disordered alloys has stimulated a great deal of theoretical and experimental effort in recent years. An outstanding contribution to the theory has been the introduction of the coherent-potential approximation (CPA) of Soven and others,¹ and its application to real physical systems. This method was first formulated within the framework of multiple-scattering theory,² and involves the determination of an effective medium whose choice is made self-consistently by requiring that the average scattering from a single real constituent in the otherwise perfect effective crystal vanishes. The hypothetical potential associated with each site of the periodic medium is usually referred to as the coherent potential, or equivalently the self-energy of the ensemble-averaged system in the single-site approximation.

In their classic paper on the electronic theory of binary alloys, Velický *et al.*³ used a single-band tight-binding model,⁴ and, for numerical purposes, a semielliptic density of states⁵ to demonstrate, among other things, that the CPA is the best of all single-site descriptions available. With respect to a Wannier basis, the model allows complete disorder in the diagonal elements

of the Hamiltonian, while the off-diagonal terms, or hopping integrals, are taken to be independent of composition and translationally invariant. The latter assumption is equivalent to the alloying of constituents with the same density of states except for the absolute positions of the bands in energy. It is an essential deficiency of the CPA that the substitution of one type of atom by another is a perturbation localized at each atom. A recent criticism⁶ of this aspect shows that self-consistency requirements on the perturbation renders the aforementioned model practically useless for real alloys. There now exists several attempts within the context of the model at generalizing the single-site CPA to include nonlocal perturbations. One of these allows for randomness in the interatomic hopping integrals. For electrons, this refinement has been investigated⁷ in terms of the locator formalism⁸ and a local-effective-medium approach⁹ reminiscent of the CPA. The extent to which these various methods are equivalent, and the question of their correctness in the low-concentration limit have been discussed in the literature.¹⁰ A more realistic case of alloying constituents having different bandwidths has been made by doing the CPA for a system of nonoverlapping muffin-tin potentials.¹¹ This modified CPA has also been applied to vibrational systems¹² with force constant and mass disorder, and to ferromagnetic binary alloys.¹³

Another important alteration of the CPA is that concerned with removing the single-site restriction. There is a well-known correlation between local clusters of impurity atoms and fine structure in the spectrum of elementary excitations.¹⁴ Characteristically, the CPA averages over these higher-order effects and only reproduces the gross features of the spectrum. Numerous studies¹⁵ of cluster effects have been carried out with both diagrammatic and multiple-scattering techniques. The effective medium is determined self-consistently by the condition that it does not scatter pairs, triplets, and higher clusters on the average. However, such considerations are not without their difficulties.¹⁶ They are not unambiguously self-consistent and give different results. More likely than not, they involve nonanalytic behavior of the average Green's function in the strong-scattering limit, and furthermore fail to satisfy the symmetry with respect to localized and bound-state expansions. Some extensions¹⁷ of the CPA are occupied with off-diagonal randomness and the formation of clusters. There is evidence (Mooyani *et al.*, Ref. 17) in pair calculations that convergence difficulties plaguing other approaches (Nickel and Butler, Ref. 16) disappear in the presence of off-diagonal randomness.

There have been a number of papers¹⁸ using the CPA to describe some actual physical systems. The first¹⁹ of these modifies the two-level model treated by Velický, Kirkpatrick, and Ehrenreich (VKE) to incorporate *sd* hybridization and orbital degeneracy and applies it to Ni-rich paramagnetic Ni-Cu alloys. The results are compatible with corresponding experimental photoemission data, but fail to represent the case of Cu-rich alloys. A reappraisal²⁰ of the crystal potential used by VKE has shown that the CPA is capable of explaining Ni-Cu alloys of arbitrary concentrations. Similar analysis has been extended to Ag-Pd alloys.²¹ A recent paper²² gives the present state of agreement between photoelectric studies of both these alloys and the CPA. It has also been reported²³ that the CPA reproduces the main features of the optical and photoemission densities of states in the Ag-Au and Cu-Au alloys over the whole composition range.

There have been a few efforts within the coherent-potential theory at going beyond the case of the binary alloy already treated so intensively over the past seven years. In a previous paper²⁴ (henceforth abbreviated as I), we investigated a three-level version of the Anderson model and established equivalence for this system between the self-consistent diagrammatic-resummation technique of Leath²⁵ and the CPA. A completely

symmetric CPA equation for the self-energy was derived and shown to be solved by an analogous binary equation when any one of the three concentrations vanished. Using a semielliptic model density of states⁵ for the reference crystal, some numerical results were presented for various one-particle quantities of interest. The basic purpose of this second in a series of papers on the equilibrium and transport properties of elementary excitations in ternary systems is to expand our previous treatment of the ternary problem along the lines described in the last paragraph of I. It should be noted that work²⁶ has been done on an *n*-component alloy of site-diagonal disorder. The ensemble-averaged Green's function is given a simple expression in the CPA and many features of the theory, such as appropriate limits, sum rules, and the criterion for the Anderson transition are discussed. Another paper²⁷ to mention in the present context is that in which the CPA is adapted to a ferromagnetic ternary alloy for the calculation of the saturation magnetization and the magnetic moment of each constituent atom.

Starting with the single-band model of ternary alloys (Sec. II A), we briefly review the general derivation of all single-site approximations using the average-Green's-function formalism and multiple-scattering theory (Sec. II B). Expressions for the self-energy are developed (Sec. II C) within the context of the CPA and the average-*T*-matrix approximation (ATA).²⁸ The latter approach does not require a self-consistent procedure and evidently is less difficult than the CPA to implement numerically, an advantage when dealing with realistic Hamiltonians.²⁹ Next (Sec. III A), we calculate the exact asymptotic behavior of the average Green's function and thereby obtain information concerning moments of the density of states and the spectral function. From these results we derive further knowledge of the exact asymptotic expansion of the self-energy and subsequently develop a family of sum rules involving the same. It is shown by direct calculation that the CPA preserves the first seven of the above-mentioned moments. Propagator-diagrammatic arguments put the highest number of exact moments given by the CPA at eight for the density of states, and seven for the spectral density. It is known from the localization theorem³⁰ that the entire spectrum can consist of two or three well-separated subbands (Sec. III B). In the singly-split-band limit the self-energy can develop a pole, while in the doubly-split-band limit it can have one or two such singularities. All of these poles are located in the region between subbands and are predicted from the exact statements. They are also found in the CPA. The existence of

these poles is an indication of the fact that these subbands are essentially independent. We continue (Sec. IV) with a detailed numerical study of the self-energy, total density of states, and the local-state density of each kind of atom, as described in the CPA. In addition to these \vec{k} -independent one-particle quantities, it is also of interest to calculate the spectral density from which we obtain information concerning the quasiparticle states of the system. Section V briefly discusses the significance of the work, and points to some possible extensions.

II. TERNARY ALLOYS

A. Anderson model of substitutional disorder

In this section we shall review the average-Green's-function formalism and the corresponding multiple-scattering theory underlying various versions of the single-site approximation essentially as given by VKE with emphasis on the substitutional disordered ternary alloy. The system consists of model atoms of types A , B , and C randomly distributed with fractional concentrations c_A , c_B , and c_C on N equivalent sites of a given regular monatomic lattice. For convenience we adopt the single-band Anderson⁴ model. A single Wannier orbital $|n\rangle$ is assigned to each site n . The one-electron Hamiltonian H for a particular configuration of atoms has the form $H = H_0 + H_1$ where

$$H_0 = \sum_n \sum_m |n\rangle t_{nm} \langle m|, \quad (2.1)$$

$$H_1 = \sum_n \epsilon_n |n\rangle \langle n|. \quad (2.2)$$

The diagonal elements ϵ_n may be regarded as atomic levels taking on one of three possible energy values ϵ_A , ϵ_B , and ϵ_C depending on whether an atom of type A , B , or C occupies the site n . The off-diagonal matrix elements are the nearest-neighbor hopping integrals t_{nm} which are specialized to be independent of the particular atoms situated at the sites n and m . Thus with respect to the Wannier representation H decomposes into a diagonal random part H_1 and an off-diagonal periodic part H_0 . The latter may be interpreted as the Hamiltonian of a perfect single-band crystal for which $\epsilon_A = \epsilon_B = \epsilon_C = 0$. The pure A , B , and C crystals are described by the Hamiltonians resulting from Eqs. (2.1) and (2.2) when ϵ_n is replaced, respectively, by ϵ_A , ϵ_B , and ϵ_C . It is of interest to extend the present form of the three-level model to include various possibilities of randomness in H_0 and thereby alloying constituents with different bandwidths. The details of that

ternary theory will be considered elsewhere.

Matrix elements of H_0 in the Bloch representation yield the dispersion relation of the tight-binding band. This property may be expressed by

$$H_0 = \alpha \sum_{\vec{k}} |\vec{k}\rangle S(\vec{k}) \langle \vec{k}|. \quad (2.3)$$

The factor α is one half the bandwidth and is an abbreviation for the product Zt , where Z is the number of first-nearest neighbors and t is the value of the hopping integral t_{nm} when n and m are nearest neighbors. The structure factor $S(\vec{k})$ describes the \vec{k} dependence of the band and is determined by the crystal symmetry. For cubic crystals $S(\vec{k})$ ranges from -1 to $+1$. A well-known feature of the single-band CPA equations is that only a knowledge of the perfect reference crystal density of states is necessary for calculating the density of states of the average alloy. This makes it possible to explore the general behavior of various properties without having to specify the detailed dependence of the hopping integral on \vec{k} .

It is convenient to express the energy levels ϵ_A , ϵ_B , and ϵ_C in units of α and to define the zero of energy such that

$$\epsilon_A = 0, \quad \epsilon_B = \alpha\beta, \quad \epsilon_C = \alpha\lambda. \quad (2.4)$$

In this way the pure A crystal Hamiltonian is made to coincide with H_0 . Since α simply scales the entire H we shall adopt energy units for which $\alpha = 1$. This normalizes the value of the hopping integral to $t = Z^{-1}$. Thus, in general, for a given choice of H_0 , the average ternary alloy is completely specified in terms of two independent dimensionless scattering parameters β and λ , and two concentrations, taken to be c_B and c_C . Our previous paper exhibited numerical examples of some quantities of interest, namely, the total density of states, partial densities of states, and the self-energy for several positive values of β and λ . Consequently, the most significant effects of alloying appeared at the top of the host band or above it. In the present work these effects are allowed to occur both at the top (or above) and the bottom (or below) of the host band.

B. Green's function and multiple-scattering theory

The macroscopic equilibrium properties of the alloy are determined by the ensemble average of the one-electron Green's function

$$G(z) = (z - H)^{-1}, \quad (2.5)$$

where z is the generalized energy. Angular brackets $\langle \dots \rangle$ will be used to denote the average over all possible equally weighted configurations of A , B , and C atoms on the lattice sites. Since

the average $\langle G(z) \rangle$ has the full crystal translational symmetry, we may in the manner of Dyson use this quantity to define the periodic electron self-energy operator $\tilde{\Sigma}(z)$ by the equation

$$\langle G(z) \rangle = G_0(z) + G_0(z) \tilde{\Sigma}(z) \langle G(z) \rangle. \quad (2.6)$$

The average alloy may be viewed as an effective medium described by $\tilde{\Sigma}(z)$, an operator which in general is complex and non-Hermitian. We let $G_0(z)$ denote the Green's function $(z - H_0)^{-1}$ of the perfect A crystal. In the Bloch representation $G_0(z)$ is diagonal and given by

$$G_0(z) = \sum_{\vec{k}} |\vec{k}\rangle [z - S(\vec{k})]^{-1} \langle \vec{k}|. \quad (2.7)$$

Using the general periodic property of averaged quantities, we may also write

$$\langle G(z) \rangle = \sum_{\vec{k}} |\vec{k}\rangle G(\vec{k}, z) \langle \vec{k}|, \quad (2.8)$$

$$\tilde{\Sigma}(z) = \sum_{\vec{k}} |\vec{k}\rangle \Sigma(\vec{k}, z) \langle \vec{k}|. \quad (2.9)$$

We have used the tilde to distinguish the operator $\tilde{\Sigma}(z)$ defined by Eq. (2.6) from the c -number quantity $\Sigma(\vec{k}, z)$ of Eq. (2.9). Of principal concern here is the \vec{k} -independent self-energy $\Sigma(z)$ of the CPA. Diagrammatically this approximation corresponds to that class of graphs associated with self-consistent single-site scatterings.²⁴ It neglects the effects of scatterings by clusters of atoms.

If there is available some starting approximation $\Omega(z)$ to $\Sigma(z)$ it is advantageous to restructure H as the sum of an auxiliary periodic part $\mathcal{H}_0 = H_0 + \Omega(z)$ and a random perturbing part $\mathcal{H}_1 = H_1 - \Omega(z)$ which provides scattering relative to \mathcal{H}_0 . In this scheme, the more judiciously we select $\Omega(z)$ the more accurate will be the approximation to $\langle G(z) \rangle$. To perform the calculation of $\langle G(z) \rangle$ it is convenient to introduce the methods of multiple-scattering theory wherein the average total scattering operator $\langle T \rangle$ may be defined by the relation

$$\langle G(z) \rangle = \mathcal{G}_0(z) + \mathcal{G}_0(z) \langle T \rangle \mathcal{G}_0(z). \quad (2.10)$$

The Green's function $\mathcal{G}_0(z) = (z - \mathcal{H}_0)^{-1}$ of the periodic crystal is equivalent to $G_0(z - \Omega(z))$. A particularly useful feature of the short-range model Hamiltonian under consideration is that its random perturbing part assumes the form of a sum of localized site contributions $\epsilon_n - \Omega(z)$. This property makes possible a closed set of equations³ which express T as the sum of contributions coming from the individual ions. The strength of the n th scatterer is given by the product of T_n , the atomic transition operator for the n th ion,

$$T_n = |n\rangle \frac{\epsilon_n - \Omega(z)}{1 - [\epsilon_n - \Omega(z)] \langle n | \mathcal{G}_0(z) | n \rangle} \langle n|, \quad (2.11)$$

and an effective wave composed of the incident wave on site n and the contribution to the scattered wave due to all other sites. The single-site approximation consists of the assumption that there exists a decomposition of the randomly perturbing potential into a sum of single atomic contributions for which the statistical correlation of T_n and the corresponding effective wave seen by the n th ion is negligible. Under these conditions,

$$\langle T \rangle = \sum_n (1 + \langle T_n \mathcal{G}_0 \rangle^{-1} \langle T_n \rangle (1 + \mathcal{G}_0 \langle T \rangle)). \quad (2.12)$$

We use Eqs. (2.6), (2.10), and (2.12) to express the single-site self-energy in the form

$$\Sigma(z) = \Omega(z) + \frac{\langle \langle n | T_n | n \rangle \rangle}{1 + \langle \langle n | T_n | n \rangle \rangle \langle n | \mathcal{G}_0(z) | n \rangle}. \quad (2.13)$$

The second term on the right-hand side of Eq. (2.13) is actually independent of the site index n . This follows from the general periodic property of average quantities and the fact that site-diagonal matrix elements of $\mathcal{G}_0(z)$ are site independent. Letting $|0\rangle$ denote the atomic orbital associated with the zeroth site, we introduce the function $\hat{F}(z)$ which in the Wannier representation is simply

$$\hat{F}(z) = \langle n | \mathcal{G}_0(z) | n \rangle = \langle 0 | \mathcal{G}_0(z) | 0 \rangle, \quad (2.14)$$

and in the Bloch representation has the expression

$$\hat{F}(z) = N^{-1} \sum_{\vec{k}} [z - S(\vec{k}) - \Omega(z)]^{-1}. \quad (2.15)$$

In a similar way the Green's function $G_0(z)$ has related to it the quantity

$$F_0(z) = \langle 0 | G_0(z) | 0 \rangle = N^{-1} \sum_{\vec{k}} [z - S(\vec{k})]^{-1}. \quad (2.16)$$

The relation between F_0 and the pure crystal density of states per atom D_0 is given by the formula

$$D_0(E) = N^{-1} \sum_{\vec{k}} \delta(E - S(\vec{k})) = -\pi^{-1} \text{Im} F_0(E + i0). \quad (2.17)$$

On combining Eqs. (2.16) and (2.17), we can formulate the useful integral relation

$$F_0(z) = \int_{-\infty}^{\infty} \frac{D_0(E) dE}{z - E}. \quad (2.18)$$

C. Average- T -matrix and coherent-potential approximations

The various ways in which Eq. (2.13) may be used have already been discussed by VKE. The self-consistent coherent-potential theory takes

the viewpoint that $\Omega(z)$ is an unknown in the problem whose value can be adjusted by requiring no average scattering from the true atom at site n when surrounded by an otherwise perfect effective medium, i.e.,

$$\langle T_n \rangle = 0. \quad (2.19)$$

Together with Eq. (2.13) this criterion leads straightaway to the equalities $\Sigma(z) = \Omega(z)$ and $\langle G(z) \rangle = \mathfrak{g}_0(z)$. More explicitly, Eq. (2.19) in the ternary case is the coherent-potential equation

$$\frac{c_B[\epsilon_B - \Sigma(z)]}{1 - [\epsilon_B - \Sigma(z)]F(z)} + \frac{c_C[\epsilon_C - \Sigma(z)]}{1 - [\epsilon_C - \Sigma(z)]F(z)} + \frac{c_A[\epsilon_A - \Sigma(z)]}{1 - [\epsilon_A - \Sigma(z)]F(z)} = 0 \quad (2.20)$$

for the determination of $\Sigma(z)$. Here we have introduced the function $F(z)$ related to the average alloy Green's function and the self-energy through the connections³¹

$$\begin{aligned} F(z) &= N^{-1} \text{Tr} \langle G(z) \rangle = \langle 0 | \langle G(z) \rangle | 0 \rangle \\ &= N^{-1} \sum_{\vec{k}} [z - S(\vec{k}) - \Sigma(z)]^{-1} = N^{-1} \sum_{\vec{k}} G(\vec{k}, z). \end{aligned} \quad (2.21)$$

$$\Sigma(z) = \Delta_1 + \frac{c_C \lambda [1 - (\beta - \Delta_1)F_0] + c_B \beta [1 - (\lambda - \Delta_1)F_0] - \Delta_1 [1 - (\beta - \Delta_1)F_0] [1 - (\lambda - \Delta_1)F_0]}{c_C \lambda [1 - (\beta - \Delta_1)F_0] F_0 + c_B \beta [1 - (\lambda - \Delta_1)F_0] F_0 + [1 - (\beta - \Delta_1)F_0] [1 - (\lambda - \Delta_1)F_0]}, \quad (2.25)$$

where $F_0 = F_0(z - \Delta_1)$. The corresponding expression for the various binary alloys formed by A , B , and C atoms follow from this result by allowing one or the other of the concentrations c_B and c_C to vanish, or by requiring their sum to equal unity. The first of these prescriptions is associated with the binary alloys AC and AB , and in the latter case leads to

$$\Sigma(z) = c_B \beta + \frac{c_B c_A \beta^2 F_0(z - c_B \beta)}{1 + \beta(c_B - c_A)F_0(z - c_B \beta)}. \quad (2.26)$$

The analogous self-energy of the AC alloy follows from the transformations $\beta \rightarrow \lambda$ and $c_B \rightarrow c_C$. The second recipe cited above provides a virtual crystal description of the BC alloy. In this instance rather than rewriting Eq. (2.25) for independent β and λ we assume

$$\epsilon_B = -\epsilon_C = \frac{1}{2} \delta, \quad (2.27)$$

and arrive at

$$\Sigma(z) = \Delta_1 + \frac{c_B c_C \delta^2 F_0(z - \Delta_1)}{1 + 2\Delta_1 F_0(z - \Delta_1)}. \quad (2.28)$$

In this case our B and C atoms coincide, re-

In view of Eq. (2.18) we also have

$$F(z) = F_0(z - \Sigma(z)) = \int_{-\infty}^{\infty} \frac{D_0(E) dE}{z - \Sigma(z) - E}. \quad (2.22)$$

In the CPA the functions $F(z)$ and $\hat{F}(z)$ are the same. For a given D_0 this approximation uses the simultaneous Eqs. (2.20) and (2.22) to secure $\Sigma(z)$ and $F(z)$. The physical significance of $F(z)$ is that

$$D(E) = -\pi^{-1} \text{Im} F(E + i0) \quad (2.23)$$

is the density of states per atom of the average alloy. Another desirable relation between these two quantities is the integral transform

$$F(z) = \int_{-\infty}^{\infty} \frac{D(E) dE}{z - E}. \quad (2.24)$$

In a non-self-consistent scheme known as the ATA, a correction to the reference self-energy is obtained by inserting $\hat{F}(z)$ and $\langle \langle n | T_n | n \rangle \rangle$ into Eq. (2.13) for a given choice of $\Omega(z)$. For example, let $\Omega(z) = \Delta_1 \equiv c_B \beta + c_C \lambda$ with \mathfrak{K}_0 then corresponding to a virtual crystal Hamiltonian. From Eqs. (2.11) and (2.13) we get

spectively, with the A and B atoms of VKE. The rigid-band approximation comes from retaining only the first term on the right-hand side of these equations for $\Sigma(z)$. As a point of comparison between the ATA and the CPA we examine the virtual-crystal limit, $0 < \beta \ll 1$ and $-1 \ll \lambda < 0$. In the former case, Eq. (2.25) yields

$$\begin{aligned} \Sigma(z) &= \Delta_1 + c_B \beta (\beta - \Delta_1) F_0(z - \Delta_1) \\ &\quad + c_C \lambda (\lambda - \Delta_1) F_0(z - \Delta_1) \end{aligned} \quad (2.29)$$

to second order in β and λ . The corresponding expression in the CPA is obtained from Eq. (2.20). To the same order, we get a self-consistent version of the above equation, namely,

$$\begin{aligned} \Sigma(z) &= \Delta_1 + c_B \beta (\beta - \Delta_1) F_0(z - \Sigma) \\ &\quad + c_C \lambda (\lambda - \Delta_1) F_0(z - \Sigma), \end{aligned} \quad (2.30)$$

where Σ in the argument of F_0 substitutes for Δ_1 . Equations (2.29) and (2.30) are straightforward generalizations of the analogous situation for the binary case which follows when c_B or c_C vanishes. We see, as in that case, that a single iteration of the CPA solution agrees with the ATA. An ex-

amination of Eq. (2.20) in the so-called atomic limit where the bandwidth vanishes and $F(z)$ is given just by $(z - \Sigma)^{-1}$ shows that $\Sigma(z)$ may then be expressed as the sum of Δ_1 plus a part with two simple poles, these being located by the solutions of a quadratic equation for z which may be seen by setting the denominator in Eq. (3.43) equal to zero. With the use of Eq. (2.29) this $\Sigma(z)$ reduces to Eq. (4.21) of VKE in the binary alloy limit $c_A = 0$.

Since the ATA is computationally much simpler than the CPA which, in fact, is the best among all single-site approximations, it is encouraging to find that the former is in remarkably good agreement with the latter, and may be considered to be a good first approximation in an iteration scheme leading to the self-consistent solution. The use of Eq. (2.13) as a means for achieving the CPA in the iterated ATA has been treated in detail by Ducastelle (Ref. 28) and Chen (Ref. 28). The problem of detailing the accuracy with which the ATA describes disordered ternary systems is deferred to a future work. For the present it will suffice to compare the CPA with rigorous properties of the single-band model which do not involve the application of the single-site assumption. This comparison is taken up in Sec. III.

III. GENERAL PROPERTIES AND COMPARISON WITH THE CPA

This section develops exact asymptotic expansions for the average Green's function and the electronic self-energy. These results provide information concerning moments and sum rules of various physical quantities which is useful in assessing the accuracy of the CPA and in discussing the singly- and doubly-split-band limits predicted by the localization theorem.

As previously mentioned, for a given choice of H_0 , the averaged ternary alloy is specified in general by β , λ , c_B , and c_C . For the purposes of this paper we shall assume that β is real and positive, while λ is real and negative. It follows from the localization theorem that the allowed range of energy eigenvalues are contained in the union of the three ranges $(-1 + \lambda, 1 + \lambda)$, $(-1, 1)$, and $(-1 + \beta, 1 + \beta)$. If the three regions are non-intersecting they are just composed of $c_C N$, $c_A N$, and $c_B N$ levels, respectively. In the present case this obtains when $\lambda < -2$ and $\beta > 2$. Should the third (first) region and that formed by the union of the first (third) and second regions be disjoint, which would be the case if $-2 < \lambda < 0$ ($\lambda < -2$) and $\beta > 2$ ($0 < \beta < 2$), then there would be $c_B N$ ($c_C N$) levels in the former and $c_A N$ and $c_C N$ ($c_A N + c_B N$) in the latter.

A. Moments and sum rules

To this exact information on the localization of the allowed energy spectrum we can add another category of exact statements, namely, that concerned with moments of the density of states, the spectral density of Bloch states and sum rules involving $\Sigma(\vec{k}, z)$. Following VKE, we define the p th moment of the density of states and the spectral density by the relations

$$\mu_p \equiv \int_{-\infty}^{\infty} E^p D(E) dE = N^{-1} \text{Tr} \langle H^p \rangle, \quad (3.1)$$

$$M_p(\vec{k}) \equiv \int_{-\infty}^{\infty} E^p \rho(\vec{k}, E) dE = \langle \vec{k} | \langle H^p \rangle | \vec{k} \rangle, \quad (3.2)$$

respectively, where $p = 0, 1, 2, \dots$. If the reference crystal density of states $D_0(E)$ is a symmetric function, as in the simple cubic and body-centered-cubic crystals, the associated moments,

$$\mu_p^{(0)} \equiv \int_{-\infty}^{\infty} E^p D_0(E) dE = N^{-1} \text{Tr} H_0^p \quad (3.3)$$

will vanish for odd values of p . The spectral density $\rho(\vec{k}, E)$, denoting the probability per unit energy that an electron having Bloch wave vector \vec{k} has energy E , is defined in elementary Green's function theory by the expression

$$\rho(\vec{k}, E) = -\pi^{-1} \text{Im} G(\vec{k}, E + i0), \quad (3.4)$$

so that

$$G(\vec{k}, z) = \int_{-\infty}^{\infty} \frac{\rho(\vec{k}, E) dE}{z - E}. \quad (3.5)$$

In the single-site approximation where $\Sigma(\vec{k}, E)$ is independent of \vec{k} this definition becomes

$$\rho(\vec{k}, E) = \pi^{-1} \frac{|\text{Im} \Sigma(E)|}{[E - S(\vec{k}) - \text{Re} \Sigma(E)]^2 + |\text{Im} \Sigma(E)|^2}. \quad (3.6)$$

Thus if a spectral peak is Lorentian its halfwidth will be given by twice the imaginary part of the self-energy. The inverse of the halfwidth multiplied by \hbar is a measure of the lifetime of an electron in the Bloch state $|\vec{k}\rangle$ in the alloy. If the imaginary part of $\Sigma(E)$ is small compared with the real part, it is then reasonable and accurate to interpret $\text{Re} \Sigma(E)$ as the shift in the energy of the electron state $|\vec{k}\rangle$.

The identities in Eqs. (3.1) and (3.2) are derivable from the boundedness of the spectrum of H . This property follows from the localization theorem which for large enough values of the energy justifies an expansion of the alloy Green's function in powers of z^{-1} ,

$$\langle G(z) \rangle = \langle (z - H^{-1}) \rangle = \sum_{p=0}^{\infty} z^{-p-1} \langle H^p \rangle. \quad (3.7)$$

A comparison of similar expansions of the right-hand sides of Eqs. (2.24) and (3.5) with the definitions $F(z) = N^{-1} \text{Tr} \langle G(z) \rangle$ and $G(\vec{k}, z) = \langle \vec{k} | \langle G(z) \rangle | \vec{k} \rangle$, after using Eq. (3.7), establishes the equalities in Eqs. (3.1) and (3.2). A straightforward procedure for calculating the average of

H^p for small p is given for the binary problem in VKE (Appendix B). Application of this simple averaging process to the ternary case for the first seven values of p yields the following expressions for $\langle H^p \rangle$ and μ_p :

$$\begin{aligned} \langle H^0 \rangle &= 1, \quad \langle H^1 \rangle = \Delta_1 + H_0, \quad \langle H^2 \rangle = \Delta_2 + 2\Delta_1 H_0 + H_0^2, \quad \langle H^3 \rangle = \Delta_3 + (2\Delta_2 + \Delta_1^2)H_0 + 3\Delta_1 H_0^2 + H_0^3, \\ \langle H^4 \rangle &= \Delta_4 + (\Delta_2 - \Delta_1^2)\mu_2^{(0)} + 2(\Delta_3 + \Delta_1\Delta_2)H_0 + 3(\Delta_2 + \Delta_1^2)H_0^2 + 4\Delta_1 H_0^3 + H_0^4, \\ \langle H^5 \rangle &= \Delta_5 + (2\Delta_3 - \Delta_1\Delta_2 - \Delta_1^3)\mu_2^{(0)} + (\Delta_2 - \Delta_1^2)\mu_3^{(0)} + [2\Delta_4 + 2\Delta_1\Delta_3 + \Delta_2^2 + 2(\Delta_2 - \Delta_1^2)\mu_2^{(0)}]H_0 \\ &\quad + (3\Delta_3 + 6\Delta_1\Delta_2 + \Delta_1^3)H_0^2 + 2(2\Delta_2 + 3\Delta_1^2)H_0^3 + 5\Delta_1 H_0^4 + H_0^5, \end{aligned} \quad (3.8)$$

$$\begin{aligned} \langle H^6 \rangle &= \Delta_6 + 3(\Delta_4 - \Delta_2\Delta_1^2)\mu_2^{(0)} + 2(\Delta_3 - \Delta_1^3)\mu_3^{(0)} + (\Delta_2 - \Delta_1^2)\mu_4^{(0)} + 2[\Delta_5 + \Delta_4\Delta_1 + \Delta_3\Delta_2 + 2(\Delta_3 - \Delta_1^3)\mu_2^{(0)} + (\Delta_2 - \Delta_1^2)\mu_3^{(0)}]H_0 \\ &\quad + 3[\Delta_4 + 2\Delta_3\Delta_1 + \Delta_2^2 + \Delta_2\Delta_1^2 + (\Delta_2 - \Delta_1^2)\mu_2^{(0)}]H_0^2 + 4(\Delta_3 + 3\Delta_2\Delta_1 + \Delta_1^3)H_0^3 + 5(\Delta_2 + \Delta_1^2)H_0^4 + 6\Delta_1 H_0^5 + H_0^6; \\ \mu_0 &= 1, \quad \mu_1 = \Delta_1, \quad \mu_2 = \Delta_2 + \mu_2^{(0)}, \quad \mu_3 = \Delta_3 + 3\Delta_1\mu_2^{(0)} + \mu_3^{(0)}, \quad \mu_4 = \Delta_4 + 2(2\Delta_2 + \Delta_1^2)\mu_2^{(0)} + 4\Delta_1\mu_3^{(0)} + \mu_4^{(0)}, \\ \mu_5 &= \Delta_5 + 5(\Delta_3 + \Delta_2\Delta_1)\mu_2^{(0)} + 5(\Delta_2 + \Delta_1^2)\mu_3^{(0)} + 5\Delta_1\mu_4^{(0)} + \mu_5^{(0)}, \\ \mu_6 &= \Delta_6 + 3(2\Delta_4 + 2\Delta_3\Delta_1 + \Delta_2^2)\mu_2^{(0)} + 2(3\Delta_3 + 6\Delta_2\Delta_1 + \Delta_1^3)\mu_3^{(0)} + 3(2\Delta_2 + 3\Delta_1^2)\mu_4^{(0)} + 6\Delta_1\mu_5^{(0)} + \mu_6^{(0)}. \end{aligned} \quad (3.9)$$

Here we have introduced a simplifying notation which recognizes that the concentrations c_B and c_C , and the scattering strengths β and λ occur in the combination $\Delta_p = c_B\beta^p + c_C\lambda^p$ ($p = 1, 2, 3, \dots$). From these results it is seen that $\langle H^p \rangle$ is a polynomial of degree p in H_0 . This quantity and μ_p are expressed in terms of Δ_l and the $\mu_l^{(0)}$ ($l \leq p$). Calculation of the diagonal matrix elements in the Bloch representation of the average H^p shows the moments $M_p(\vec{k})$ to be the same function as the $\langle H^p \rangle$, with H_0 replaced everywhere by $S(\vec{k})$.

The average Green's function may be used to determine an effective Hamiltonian H_{eff} by means

of the statement

$$\langle G(z) \rangle = \langle (z - H)^{-1} \rangle = (z - H_{\text{eff}})^{-1}. \quad (3.10)$$

The effective Hamiltonian has the full crystal translational symmetry and is diagonal in the \vec{k} representation

$$H_{\text{eff}}(z) = \sum_{\vec{k}} |\vec{k}\rangle [S(\vec{k}) - \Sigma(\vec{k}, z)] \langle \vec{k}|. \quad (3.11)$$

Paralleling the steps outlined in VKE for determining the asymptotic expansion of H_{eff} , we obtain

$$\begin{aligned} H_{\text{eff}}(z) &= \Delta_1 + H_0 + (\Delta_2 - \Delta_1^2)z^{-1} + (\Delta_3 - 2\Delta_2\Delta_1 + \Delta_1^3)z^{-2} + [\Delta_4 - 2\Delta_3\Delta_1 + 3\Delta_2\Delta_1^2 - \Delta_2^2 - \Delta_1^4 + (\Delta_2 - \Delta_1^2)\mu_2^{(0)}]z^{-3} \\ &\quad + [\Delta_5 - 2\Delta_4\Delta_1 - 2\Delta_3\Delta_2 + 3\Delta_3\Delta_1^2 + 3\Delta_2^2\Delta_1 - 4\Delta_2\Delta_1^3 + \Delta_1^5 + (2\Delta_3 - 3\Delta_2\Delta_1 + \Delta_1^3)\mu_2^{(0)} + (\Delta_2 - \Delta_1^2)\mu_3^{(0)}]z^{-4} \\ &\quad + [\Delta_6 - 2\Delta_5\Delta_1 + 3\Delta_4\Delta_1^2 - 4\Delta_3\Delta_1^3 + 5\Delta_2\Delta_1^4 - 2\Delta_2(\Delta_4 - 3\Delta_3\Delta_1 + 3\Delta_2\Delta_1^2) - \Delta_3^2 + \Delta_2^3 - \Delta_1^6 + (3\Delta_4 - 4\Delta_3\Delta_1 + 4\Delta_2\Delta_1^2 \\ &\quad - 2\Delta_2^2 - \Delta_1^4)\mu_2^{(0)} + 2(\Delta_3 - \Delta_2\Delta_1)\mu_3^{(0)} + (\Delta_2 - \Delta_1^2)\mu_4^{(0)}]z^{-5} + \dots \end{aligned} \quad (3.12)$$

The self-energy is now determined to the same order by using this expression for H_{eff} to form the matrix element $\langle \vec{k} | H_{\text{eff}} | \vec{k} \rangle$ which according to Eq. (3.11) is equivalent to $S(\vec{k}) + \Sigma(\vec{k}, z)$. We find

$$\begin{aligned} \Sigma(\vec{k}, z) &= \Delta_1 + (\Delta_2 - \Delta_1^2)z^{-1} + (\Delta_3 - 2\Delta_2\Delta_1 + \Delta_1^3)z^{-2} + [\Delta_4 - 2\Delta_3\Delta_1 + 3\Delta_2\Delta_1^2 - \Delta_2^2 - \Delta_1^4 + (\Delta_2 - \Delta_1^2)\mu_2^{(0)}]z^{-3} \\ &\quad + [\Delta_5 - 2\Delta_4\Delta_1 - 2\Delta_3\Delta_2 + 3\Delta_3\Delta_1^2 + 3\Delta_2^2\Delta_1 - 4\Delta_2\Delta_1^3 + \Delta_1^5 + (2\Delta_3 - 3\Delta_2\Delta_1 + \Delta_1^3)\mu_2^{(0)} + (\Delta_2 - \Delta_1^2)\mu_3^{(0)}]z^{-4} \\ &\quad + [\Delta_6 - 2\Delta_5\Delta_1 + 3\Delta_4\Delta_1^2 - 4\Delta_3\Delta_1^3 + 5\Delta_2\Delta_1^4 - 2\Delta_2(\Delta_4 - 3\Delta_3\Delta_1 + 3\Delta_2\Delta_1^2) - \Delta_3^2 + \Delta_2^3 - \Delta_1^6 \\ &\quad + (3\Delta_4 - 4\Delta_3\Delta_1 + 4\Delta_2\Delta_1^2 - 2\Delta_2^2 - \Delta_1^4)\mu_2^{(0)} + 2(\Delta_3 - \Delta_2\Delta_1)\mu_3^{(0)} + (\Delta_2 - \Delta_1^2)\mu_4^{(0)}]z^{-5} + \dots \end{aligned} \quad (3.13)$$

The coefficients of z^{-l} ($1 \leq l \leq 5$) in the expansion of H_{eff} are simply c numbers, while the self-energy is independent of \vec{k} to the same order. An important consequence of the analyticity of $H_{\text{eff}}(z)$ in both half planes and the behavior of $\Sigma(\vec{k}, z)$ as $|z| \rightarrow \infty$ is the Kramers-Kronig formula

$$\Sigma(\vec{k}, z) = \Delta_1 + \pi^{-1} \int_{-\infty}^{\infty} \frac{dE}{z - E} \text{Im} \Sigma(\vec{k}, E + i0). \quad (3.14)$$

This dispersion relation furnishes a series of sum rules, the lowest two of which are

$$\int_{-\infty}^{\infty} \text{Im} \Sigma(\vec{k}, E + i0) dE = -\pi(\Delta_2 - \Delta_1^2), \quad (3.15)$$

$$\int_{-\infty}^{\infty} E \text{Im} \Sigma(\vec{k}, E + i0) dE = -\pi(\Delta_3 - 2\Delta_2\Delta_1 + \Delta_1^3). \quad (3.16)$$

All of these results for $\langle H^p \rangle$, μ_p , $M_p(\vec{k})$, $H_{\text{eff}}(z)$, and $\Sigma(\vec{k}, z)$ reduce to the binary alloy forms of VKE by simultaneously letting $c_A = 0$ and allowing Eq. (2.27) to hold.

The previous statements made about the localization of the spectrum and the asymptotic behavior of $G(\vec{k}, z)$ and the density of states are not only of intrinsic interest but also are of value in judging the predictions of approximate treatments of the ternary alloy problem. At first we wish to examine the CPA vis-à-vis the latter category of exact results. For this purpose we recast the CPA equation, Eq. (2.20), into the form

$$\Sigma = \Delta_1 + (\beta + \lambda + \Delta_1)F\Sigma - 2F\Sigma^2 - \beta\lambda(c_B + c_C)F - \beta\lambda F^2\Sigma + (\beta + \lambda)F^2\Sigma^2 - F^2\Sigma^3, \quad (3.17)$$

where $F = F(z)$ and $\Sigma = \Sigma(z)$. On the grounds that Σ approaches Δ_1 and $(z - \Sigma)$ diverges as $|z| \rightarrow \infty$, we expand, in that limit, the right-hand side of Eq. (2.22) as an infinite power series of $(z - \Sigma)^{-1}$ with $\mu_p^{(0)}$ as the coefficient of $(z - \Sigma)^{-p-1}$. Writing the self-energy as

$$\Sigma(z) = \Delta_1 + \sigma_1 z^{-1} + \sigma_2 z^{-2} + \sigma_3 z^{-3} + \sigma_4 z^{-4} + \sigma_5 z^{-5} + O(z^{-6}), \quad (3.18)$$

and inserting it into this expression of Eq. (2.22), we get $F(z)$ as a power series in z^{-1} . On substituting this result into the left-hand side of Eq. (2.24) and expanding its right-hand side in powers of z^{-1} , we are led to equate the coefficient of z^{-p-1} in the series for $F(z)$ with the moment μ_p . In view of Eqs. (2.21) and (3.18), we may similarly develop $G(\vec{k}, z)$ as a power series, and matching this against the one obtained by expanding the right-hand side of Eq. (3.5) find, with the aid of Eq. (3.2), that the coefficient of z^{-p-1} in the series for $G(\vec{k}, z)$ corresponds to the moment $M_p(k)$. The unknown quantities σ_p in these expressions for

the moments are found by inserting Eq. (3.18) and the above-mentioned series for $F(z)$ into Eq. (3.17) and comparing coefficients of z^{-p} on both sides. This straightforward but quite laborious process yields an expression for σ_p ($1 \leq p \leq 5$) which agrees with the coefficient of z^{-p} in Eq. (3.13). In this way we prove by direct calculation that $\Sigma(z)$ of the CPA reproduces to order z^{-5} the exact $\Sigma(\vec{k}, z)$ as $|z| \rightarrow \infty$. Therefore, the CPA preserves the first seven moments of the density of states and spectral density. Obviously, this conclusion is also valid for binary alloys which are now simply limiting cases of the present system and extends the work of VKE where the number of exact moments given by the CPA is at least six. The question of the highest number of moments given correctly by this approximation has been considered for the binary case by Blackman, Esterling, and Berk (Ref. 7), who use propagator—and locator—diagrammatic arguments to prove that the CPA preserves the first eight moments (μ_0, \dots, μ_7) of the density of states and the first seven moments (M_0, \dots, M_6) of the spectral density. These authors show how a lowest-order non-single-site-type graph in the diagrammatic expansion of the alloy Green's function causes error in M_7 and μ_8 of the CPA. Applying similar diagrammatic considerations to the ternary case, we find that this failure of the CPA will also begin to arise here at the same moments.

B. Singly- and doubly-split-band limits

We now go on to derive a number of properties of the ternary alloy in the singly- and doubly-split-band limits. The former will be obtained by holding ϵ_C fixed, and not too different from $\epsilon_A (= 0)$, while allowing ϵ_B to become large enough for the appearance of two well-separated subbands. The total density of states may then be expressed as the sum of two parts, called $D_\alpha(E)$ and $D_\omega(E)$, centered around the atomic level ϵ_B and the center of gravity $\epsilon = (c_C \epsilon_C + c_A \epsilon_A)(c_C + c_A)^{-1}$, respectively. On the other hand, the doubly-split-band limit will, for analytical convenience, be realized by using Eq. (2.27) and letting δ become large enough for the appearance of three well-separated subbands. In this case the total density of states is the sum of three terms $D_\kappa(E)$, $D_\nu(E)$, and $D_\tau(E)$ centered about the corresponding levels ϵ_A , ϵ_B , and ϵ_C . If the atomic level ϵ_B is permitted to increase without limit the subbands α and ω are associated entirely with B atoms and the AC binary alloy, respectively. Similarly, for the κ band with A atoms, the ν band with B atoms and the τ band with C atoms as $\delta \rightarrow \infty$.

In the singly-split-band case, the moments of the density of states within the two subbands are

defined by

$$\mu_p^\alpha = \int_{-\infty}^{\infty} (E - \epsilon_B)^p D_\alpha(E) dE, \quad (3.19)$$

$$\mu_p^\omega = \int_{-\infty}^{\infty} (E - \epsilon)^p D_\omega(E) dE. \quad (3.20)$$

They are connected to the moments μ_p of the total density of states by the infinite set of equations

$$\mu_p = \sum_{l=0}^p \binom{p}{l} (\epsilon_B^l \mu_{p-l}^\alpha + \epsilon^l \mu_{p-l}^\omega), \quad (3.21)$$

solved in practice by truncation. However, if the first n equations are treated separately from the rest, there arises the difficulty of having twice as many $\mu_p^{\alpha,\omega}$ as μ_p . Fortunately, this feature is absent from the present consideration since only the leading powers of β^{-1} are important. Thus by systematically neglecting terms of order—say, β^{-3} and higher, we obtain

$$\begin{aligned} \mu_0^\alpha &= c_B + O(\beta^{-3}), & \mu_0^\omega &= c_A + c_C + O(\beta^{-3}), \\ \mu_1^\alpha &= c_B(c_A + c_C)\mu_2^{(0)}\beta^{-1} + O(\beta^{-2}), \\ \mu_1^\omega &= -c_B(c_A + c_C)\mu_2^{(0)}\beta^{-1} + O(\beta^{-2}), \\ \mu_2^\alpha &= c_B^2\mu_2^{(0)} + O(\beta^{-1}), \\ \mu_2^\omega &= (c_A + c_C)^2\mu_2^{(0)} + c_A c_C (c_A + c_C)^{-1}\lambda^2 + O(\beta^{-1}). \end{aligned} \quad (3.22)$$

Because of the localization theorem the results for the zero moments could have been anticipated; μ_0^α and μ_0^ω are just the weights of the subbands. The moments μ_1^α and μ_1^ω describe the mean shift from the level ϵ_B and the center of gravity ϵ . The fourth and fifth lines in Eqs. (3.22) provide a measure of the effective widths of the subbands. It is of interest to study the variation of these widths as a function of the concentrations and λ for fixed but large β . The latter parameter is taken so large that shifts in the subbands are negligible. It should be remembered that the magnitude of λ is considered to be much less than unity. We assume the dependence of the subbands on concentrations and λ to be describable by simple affine transformations:

$$\begin{aligned} M_0^\alpha(\vec{k}) &= c_B + 2c_B(c_A + c_C)S(\vec{k})\beta^{-1} - \{3c_B(c_A + c_C)(c_B - c_A - c_C)[S^2(\vec{k}) - \mu_2^{(0)}] - 2c_B c_C \lambda S(\vec{k})\}\beta^{-2} + O(\beta^{-3}), \\ M_1^\alpha(\vec{k}) &= c_B S(\vec{k}) + \{3c_B^2(c_A + c_C)[S^2(\vec{k}) - \mu_2^{(0)}] + c_B(c_A + c_C)\mu_2^{(0)}\}\beta^{-1} + O(\beta^{-2}), \\ M_2^\alpha(\vec{k}) &= c_B^2(c_A + c_C)\mu_2^{(0)} + c_B^3 S^2(\vec{k}) + O(\beta^{-1}), \end{aligned} \quad (3.30)$$

$$\begin{aligned} M_0^\omega(\vec{k}) &= c_A + c_C - 2c_B(c_A + c_C)S(\vec{k})\beta^{-1} + \{3c_B(c_A + c_C)(c_B - c_A - c_C)[S^2(\vec{k}) - \mu_2^{(0)}] - 2c_B c_C \lambda S(\vec{k})\}\beta^{-2} + O(\beta^{-3}), \\ M_1^\omega(\vec{k}) &= (c_A + c_C)^2 S(\vec{k}) - \{3c_B(c_A + c_C)^2[S^2(\vec{k}) - \mu_2^{(0)}] + c_B(c_A + c_C)\mu_2^{(0)}\}\beta^{-1} + O(\beta^{-2}), \\ M_2^\omega(\vec{k}) &= c_B(c_A + c_C)^2\mu_2^{(0)} + (c_A + c_C)^3 S^2(\vec{k}) + c_A c_C \lambda^2 (c_A + c_C)^{-1} + O(\beta^{-1}). \end{aligned}$$

$$D_\alpha(E|c_B) = \eta_1 D_0[(E - \beta)/\eta_2], \quad (3.23)$$

$$D_\omega(E|c_A, c_C, \lambda) = \xi_1 D_0[(E - \epsilon)/\xi_2], \quad (3.24)$$

where D_0 is the pure crystal density of states given in Eq. (2.17). It follows that Eqs. (3.22) are satisfied only if

$$\eta_1 = \eta_2 = c_B^{1/2}, \quad (3.25)$$

$$\xi_1 = (c_A + c_C)^{1/2} [1 + c_A c_C \lambda^2 / (c_A + c_C)^3 \mu_2^{(0)}]^{-1/2}, \quad (3.26)$$

$$\xi_2 = (c_A + c_C)^{1/2} [1 + c_A c_C \lambda^2 / (c_A + c_C)^3 \mu_2^{(0)}]^{1/2}. \quad (3.27)$$

These results provide a description of the behavior of the subbands in terms of concentrations, λ and $\mu_2^{(0)}$. According to Eq. (3.25) the height and width of the α band vary as $c_B^{1/2}$. By contrast, Eqs. (3.26) and (3.27) show, for non-negligible λ^2 , that the corresponding dimensions of the ω band do not simply scale as $(c_A + c_C)^{1/2}$. For example, an increase in λ^2 for fixed concentrations causes an increase in the width and a decrease in the height of this band. In the limit $\lambda^2 = \mu_2^{(0)} c_B (c_A + c_C)^2 (c_A c_C)^{-1}$ the ω band completely fills the region permitted by the localization theorem. For each band the product of height and width is proportional to its weight. In the limits $c_A = 0$ and $c_C = 0$, the expressions in Eqs. (3.25)–(3.27) pertain to the split-band limit of the binary alloy formed by B and C atoms, and B and A atoms, respectively.

The moments of the spectral density in the singly-split-band limit are defined by

$$M_p^\alpha(\vec{k}) = \int_{-\infty}^{\infty} (E - \epsilon_B)^p \rho_\alpha(\vec{k}, E) dE, \quad (3.28)$$

$$M_p^\omega(\vec{k}) = \int_{-\infty}^{\infty} (E - \epsilon)^p \rho_\omega(\vec{k}, E) dE. \quad (3.29)$$

As in the foregoing treatment of the moments of the subband density of states, one finds an infinite set of equations connecting the M_p and the $M_p^{\alpha,\omega}$. Proceeding in the same manner, we find

In going on to discuss some features of the spectral function, we shall assume that the separation between subbands is so large that only the β -independent terms in Eqs. (3.30) are significant. From the zeroth moments we then infer that an electron in Bloch state $|\tilde{\mathbf{k}}\rangle$ has the probabilities c_B and $c_A + c_C$, respectively, of occupying B -atom, and A - and C -atom sites. The centers of gravity $E_{\alpha,\omega}(\tilde{\mathbf{k}})$ of the spectral functions $\rho_{\alpha,\omega}(\tilde{\mathbf{k}}, E)$ are located by the first-order moments according to

$$\begin{aligned} E_{\alpha}(\tilde{\mathbf{k}}) &= \beta + M_1^{\alpha}(\tilde{\mathbf{k}})/M_0^{\alpha}(\tilde{\mathbf{k}}) = \beta + c_B S(\tilde{\mathbf{k}}), \\ E_{\omega}(\tilde{\mathbf{k}}) &= \epsilon + M_1^{\omega}(\tilde{\mathbf{k}})/M_0^{\omega}(\tilde{\mathbf{k}}) = \epsilon + (c_A + c_C)S(\tilde{\mathbf{k}}). \end{aligned} \quad (3.31)$$

An approximate measure of the extent to which the α and ω bands are spread about their centers of gravity is given by the $\tilde{\mathbf{k}}$ -independent quantities

$$\begin{aligned} & \{M_2^{\alpha}(\tilde{\mathbf{k}})/M_0^{\alpha}(\tilde{\mathbf{k}}) - [M_1^{\alpha}(\tilde{\mathbf{k}})/M_0^{\alpha}(\tilde{\mathbf{k}})]^2\}^{1/2} \\ &= [c_B(c_A + c_C)\mu_2^{(0)}]^{1/2}, \\ & \{M_2^{\omega}(\tilde{\mathbf{k}})/M_0^{\omega}(\tilde{\mathbf{k}}) - [M_1^{\omega}(\tilde{\mathbf{k}})/M_0^{\omega}(\tilde{\mathbf{k}})]^2\}^{1/2} \\ &= [c_A c_C (c_A + c_C)^{-2} \lambda^2 + c_B (c_A + c_C)\mu_2^{(0)}]^{1/2}. \end{aligned} \quad (3.32)$$

A few limiting cases of these results are worthy of note. To begin with, as c_A and c_C recede down to zero, Eqs. (3.31) and (3.32) become appropriate for subbands of binary alloys formed with B and C atoms and B and A atoms, respectively. The subsequent behavior of these subbands as the remaining concentrations (c_B and c_C or c_B and c_A) separately approach zero or unity has already been covered by VKE. Alternatively, as the concentration of B atoms tends to zero, so also does the shift and linewidth of the α band and consequently, a sharp isolated impurity line appears around ϵ_B . At the same time, the center of gravity of the spectral function $\rho_{\omega}(\tilde{\mathbf{k}}, E)$ converges to the virtual crystal eigenvalue $\epsilon + S(\tilde{\mathbf{k}})$, while its linewidth goes roughly as $\lambda(c_A c_C)^{1/2}$. When $c_B \rightarrow 1$, the ω and α bands are identified, respectively, by a sharp impurity line centered at ϵ and the sharp Bloch eigenstates of the B crystal.

In the doubly-split-band limit, we denote the moments of the subband densities of states by

$$\mu_p^{\kappa} = \int_{-\infty}^{\infty} (E - \epsilon_A)^p D_{\kappa}(E) dE, \quad (3.33)$$

$$\mu_p^{\nu} = \int_{-\infty}^{\infty} (E - \epsilon_B)^p D_{\nu}(E) dE, \quad (3.34)$$

$$\mu_p^{\tau} = \int_{-\infty}^{\infty} (E - \epsilon_C)^p D_{\tau}(E) dE. \quad (3.35)$$

The infinite set of equations relating these quantities and moments μ_p is given by

$$\mu_p = \mu_p^{\kappa} + \sum_{i=0}^p \binom{p}{i} (\epsilon_B^i \mu_{p-i}^{\nu} + \epsilon_C^i \mu_{p-i}^{\tau}). \quad (3.36)$$

To solve for the $\mu_p^{\kappa, \nu, \tau}$, we proceed as before and adopt a truncation scheme systematically neglecting terms of order δ^{-3} and higher. This yields seven equations expressing the known moments μ_0, \dots, μ_6 in terms of the nine unknowns $\mu_0^{\kappa, \nu, \tau}, \dots, \mu_2^{\kappa, \nu, \tau}$. Because the moments $\mu_0^{\kappa, \nu, \tau}$ simply correspond to the weights of the subbands we expect from the localization theorem that they equal the concentrations c_A , c_B , and c_C . This fact is used to reduce the number of equations and unknowns to six with the solutions

$$\begin{aligned} \mu_0^{\kappa} &= c_A + O(\delta^{-3}), \\ \mu_0^{\nu} &= c_B + O(\delta^{-3}), \\ \mu_0^{\tau} &= c_C + O(\delta^{-3}), \\ \mu_1^{\kappa} &= -c_A c_B \mu_2^{(0)} \left(\frac{\delta}{2}\right)^{-1} + c_A c_C \mu_2^{(0)} \left(\frac{\delta}{2}\right)^{-1} + O(\delta^{-2}), \\ \mu_1^{\nu} &= c_B c_A \mu_2^{(0)} \left(\frac{\delta}{2}\right)^{-1} + c_B c_C \mu_2^{(0)} \delta^{-1} + O(\delta^{-2}), \\ \mu_1^{\tau} &= -c_C c_A \mu_2^{(0)} \left(\frac{\delta}{2}\right)^{-1} - c_C c_B \mu_2^{(0)} \delta^{-1} + O(\delta^{-2}), \\ \mu_2^{\kappa} &= c_A^2 \mu_2^{(0)} + O(\delta^{-1}), \\ \mu_2^{\nu} &= c_B^2 \mu_2^{(0)} + O(\delta^{-1}), \\ \mu_2^{\tau} &= c_C^2 \mu_2^{(0)} + O(\delta^{-1}). \end{aligned} \quad (3.37)$$

It is hardly necessary to dwell on the interpretation of these results. The fourth through ninth lines describe the mean shifts from the atomic levels and the effective widths of the subbands. Note that the shift associated with any two levels increases the gap between corresponding subbands. This feature is also present in the previous case of two subbands and, as noted similarly by VKE, is consistent with the repulsion of energy levels well known from perturbation theory. If, as before, we neglect the shifts and assume a two parameter model, it is found that heights and widths of the subbands κ , ν and τ scale, respectively, as the square root of c_A , c_B and c_C . Also, it is immediately obvious that Eqs. (3.37) reduce to the binary-alloy split-band situation when any one of the concentrations vanishes.

We conclude this discussion of the doubly split regime by briefly considering the moments $M_p^{\kappa, \nu, \tau}(\tilde{\mathbf{k}})$ of the spectral density. These quantities are defined by integrals of the type shown in Eqs. (3.28) and (3.29) with corresponding spectral functions $\rho_{\kappa, \nu, \tau}(\tilde{\mathbf{k}}, E)$, and origins of energy shifted to the positions ϵ_A , ϵ_B , and ϵ_C . Making use of the fact that the total spectral density $\rho(\tilde{\mathbf{k}}, E)$ is

now given by the sum of three parts, we can construct, as before, an infinite set of equations connecting the $M_p^{\kappa, \nu, \tau}(\vec{k})$ with the $M_p(\vec{k})$:

$$M_p(\vec{k}) = M_p^{\kappa}(\vec{k}) + \sum_{l=0}^p \binom{p}{l} [\epsilon_B^l M_{p-l}^{\nu}(\vec{k}) + \epsilon_C M_{p-l}^{\tau}(\vec{k})]. \quad (3.38)$$

A truncation approach neglecting terms of order δ^{-3} and higher leads to seven equations giving the moments M_0, \dots, M_6 in terms of the nine unknowns $M_0^{\kappa, \nu, \tau}, \dots, M_2^{\kappa, \nu, \tau}$. It is readily verified with the relationship $\mu_p^{\kappa, \nu, \tau} = N^{-1} \sum_{\vec{k}} M_p^{\kappa, \nu, \tau}(\vec{k})$ that these equations are consistent with Eqs. (3.37), however, in view of the lack of expressions for M_7 and M_8 , we are not in a position to calculate solutions to this order. Instead, we omit terms of order δ^{-2} and higher, and derive the zeroth and first moments of the spectral density. Doing this results in

$$\begin{aligned} M_0^{\kappa}(\vec{k}) &= c_A + 2c_A c_C S(\vec{k}) \left(\frac{\delta}{2}\right)^{-1} \\ &\quad - 2c_A c_B S(\vec{k}) \left(\frac{\delta}{2}\right)^{-1} + O(\delta^{-2}), \\ M_0^{\nu}(\vec{k}) &= c_B + 2c_B c_A S(\vec{k}) \left(\frac{\delta}{2}\right)^{-1} \\ &\quad + 2c_B c_C S(\vec{k}) \delta^{-1} + O(\delta^{-2}), \\ M_0^{\tau}(\vec{k}) &= c_C - 2c_C c_A S(\vec{k}) \left(\frac{\delta}{2}\right)^{-1} \\ &\quad - 2c_C c_B S(\vec{k}) \delta^{-1} + O(\delta^{-2}), \\ M_1^{\kappa}(\vec{k}) &= c_A^2 S(\vec{k}) + O(\delta^{-1}), \\ M_1^{\nu}(\vec{k}) &= c_B^2 S(\vec{k}) + O(\delta^{-1}), \\ M_1^{\tau}(\vec{k}) &= c_C^2 S(\vec{k}) + O(\delta^{-1}). \end{aligned} \quad (3.39)$$

The corresponding moments of the subband densities of states consistent with Eqs. (3.39) are obtained from the first six equations following from Eq. (3.36). In this case the weights of the subbands are written as in the first three lines of Eqs. (3.37) with corrections of $O(\delta^{-2})$. The mean shifts have zero value with corrections of order δ^{-1} .

These results and those of Eqs. (3.30) suffice to show that $\Sigma(\vec{k}, z)$ may have a pole between adjacent

subbands in the doubly-split-band limit, and one pole in the singly-split-band limit. The existence of these singular points is a manifestation of the band splitting. In view of the relationship between $G(\vec{k}, z)$ and $\Sigma(\vec{k}, z)$, following from Eqs. (2.8), (3.10), and (3.11), it is convenient to first find the zeros of the former function as these occur for finite z where the latter has poles. We proceed with the singly-split-band case by making use of the decomposition $\rho = \rho_\alpha + \rho_\omega$ to express Eq. (3.5) as

$$G(\vec{k}, z) = \sum_{p=0}^{\infty} [M_p^{\alpha}(\vec{k})(z - \epsilon_B)^{-p-1} + M_p^{\omega}(\vec{k})(z - \epsilon)^{-p-1}]. \quad (3.40)$$

Let us now suppose that β is large, the magnitude of λ is small, and the energy is very remote from both subbands. For this situation, it is only necessary to consider the first few terms of Eq. (3.40) with the moments given by Eqs. (3.30). It is then readily shown that $G(\vec{k}, z)$ has a zero located between the subbands at $E_0 = (c_A + c_C)\beta + c_B\epsilon$. This statement is exact to order β^{-2} . In the neighborhood of this point $G(\vec{k}, z)$ is given by

$$G(\vec{k}, z) \approx - \frac{z - \beta(c_A + c_C) - \lambda c_B c_C / (c_A + c_C)}{c_B(c_A + c_C)\beta^2 - 2\beta\lambda c_B c_C - \mu_2^{(0)}}. \quad (3.41)$$

The denominator in this expression is determined by calculating the derivative of $G(\vec{k}, z)$ at its zero point. In arriving at this result, we assume that β , βc_A , βc_B , and βc_C are all much greater than unity, while the magnitudes of λ , λc_A , λc_B , and λc_C are much less than unity. We conclude that $\Sigma(\vec{k}, z)$ may be represented as the sum of a regular part and a pole part, the latter given by the \vec{k} -independent form

$$\Sigma_{\text{pole}}(\vec{k}, z) \approx \frac{c_B(c_A + c_C)\beta^2 - 2\lambda\beta c_B c_C - \mu_2^{(0)}}{z - \beta(c_A + c_C) - \lambda c_B c_C / (c_A + c_C)}. \quad (3.42)$$

The way to prove this result in the CPA begins with an expansion of $F(z)$ in terms of inverse powers of $\Sigma(z)$ obtained from Eq. (2.22). This expansion is inserted into the right-hand side of Eq. (3.17) which is then written to order $\Sigma^{-2}(z)$ and subsequently solved by

$$\Sigma(z) \approx \frac{-2z^3 + (2\beta + 2\lambda - \Delta_1)z^2 - [\beta\lambda(1 + c_A) + 2\mu_2^{(0)}]z + (\beta + \lambda - \Delta_1)\mu_2^{(0)}}{z^2 - (\beta + \lambda - \Delta_1)z + \beta\lambda c_A}. \quad (3.43)$$

In the present case where the energies are far removed from both subbands and where $\beta \gg 1$ and $|\lambda| \ll 1$ only the positive square root solution of the quadratic equation for z , that arises when the denominator in Eq. (3.43) is set equal to zero, provides $\Sigma(z)$ with a pole between the subbands at E_0 . This is shown by expanding the square root in powers of (λ/β) and neglecting terms of order $(\lambda/\beta)^2$ and higher. Expressing the denominator in Eq. (3.43) as the product of two factors, one of which is $(z - E_0)$, and evaluating the other factor together with the numerator at E_0 , we find that $\Sigma(z)$ of (3.43) becomes identical with Eq. (3.42). It is seen from Eqs. (2.21) and (2.23) that the positive definite density of states requires the imaginary part of $\Sigma(E + i0)$ to be less than or equal to zero. This provides the necessary condition,

$$c_B(c_A + c_C)\beta^2 - 2\lambda\beta c_B c_C \geq \mu_2^{(0)}, \quad (3.44)$$

for the existence of the pole for $\Sigma(z)$ in the singly-split-band case.

Given the circumstances for the presence of a pole in $\Sigma(\vec{k}, E)$, we are able to show to order β^{-2} , following VKE, that the contributions of the individual subbands α and ω to the sum rules in Eqs. (3.15) and (3.16) are independent of β and λ and given by $-\pi(c_A + c_C)\mu_2^{(0)}$ and $-\pi c_B \mu_2^{(0)}$, respectively. The derivation of these results also includes neglecting terms of order λ^2 and λ^3 on the right-hand side of Eqs. (3.15) and (3.16). As expected, the damping in the ω (α) subband and the concentration c_B ($c_A + c_C$) decrease simultaneously. Quite similarly to VKE, our proof of this behavior breaks down when c_B or $c_A + c_C$ is too small. Of course, it continues to hold in the binary alloy limits $c_A \rightarrow 0$ or $c_C \rightarrow 0$ for which $E_0 \rightarrow c_C \epsilon_B + c_B \epsilon_C$ or $E_0 \rightarrow c_A \epsilon_B$.

The doubly-split-band limit is treated in the same way as the singly-split-band case. In place of Eq. (3.40) we now have

$$G(\vec{k}, z) = \sum_{p=0}^{\infty} [M_p^{\kappa}(\vec{k})(z - \epsilon_A)^{-p-1} + M_p^{\nu}(\vec{k})(z - \epsilon_B)^{-p-1} + M_p^{\tau}(\vec{k})(z - \epsilon_C)^{-p-1}], \quad (3.45)$$

where $\rho = \rho_{\kappa} + \rho_{\nu} + \rho_{\tau}$ has been used. As before, we consider conditions for which δ is large and the energies of interest are so far removed from all three subbands that it is sufficient to employ the first couple of terms of Eq. (3.45) with the moments given by Eqs. (3.39). From this we can establish to accuracy δ^{-1} the existence of two values of the energy,

$$E_{\pm} = \frac{1}{4}(\delta) \{ (c_C - c_B) \pm [(c_C - c_B)^2 + 4c_A]^{1/2} \} \equiv \frac{1}{4}(\delta) \epsilon_{\pm}, \quad (3.46)$$

at which $G(\vec{k}, z)$ vanishes; E_+ (E_-) lies on the real energy axis between the subbands κ and ν (τ). Thus $\Sigma(\vec{k}, z)$ has poles at E_{\pm} for any \vec{k} . The same fact is immediately evident in the CPA by noticing that the denominator of the right-hand side of Eq. (3.43) vanishes at these energies. Since the present solution is exact only to order δ^{-1} , we do not expect the residues of $\Sigma(\vec{k}, z)$ and $\Sigma(z)$ at the poles to agree as in the previous case of the singly split band. Indeed, such agreement is already absent in the binary alloy limit $c_A \rightarrow 0$ where $\Sigma(z)$ of Eq. (3.43) takes on the VKE form

$$\Sigma(z) \approx \frac{c_B c_C \delta^2 - \mu_2^{(0)}}{z + \frac{1}{2} \delta (c_B - c_C)}, \quad (3.47)$$

while the corresponding expression for $\Sigma(\vec{k}, z)$ lacks the $\mu_2^{(0)}$ term appearing in the numerator. For this reason we do not proceed further within the present solution to construct the exact $\Sigma(\vec{k}, z)$ in the neighborhood of E_{\pm} . However, with Eq. (3.43) at hand, it is possible to determine the structure of $\Sigma(z)$ in the vicinity of these poles. This is done by giving $\Sigma(z)$ the expression

$$\Sigma(z) \approx \frac{\{(\frac{1}{4} \delta^2)[1 - (c_B - c_C)^2] - 2\mu_2^{(0)}\} z + (\frac{1}{2} \delta)(c_B - c_C)[(\frac{1}{2} \delta)^2 c_A - \mu_2^{(0)}]}{(z - E_+)(z - E_-)}, \quad (3.48)$$

where the numerator in Eq. (3.48) and the appropriate factor in the denominator are to be evaluated at E_+ or E_- according as we seek $\Sigma(z)$ near E_+ or E_- . Note that Eq. (3.48) reproduces Eq. (3.47) in the limit as c_A vanishes and z approaches $(\frac{1}{2} \delta)(c_C - c_B)$. Again, we obtain the necessary criteria,

$$\pm (\epsilon_+ - \epsilon_-)^{-1} [(\frac{1}{8} \delta^2)(c_A + 2c_B)(c_A + 2c_C)\epsilon_{\pm} + (c_C - c_B - \epsilon_{\pm})\mu_2^{(0)} - (\frac{1}{4} \delta^2)c_A(c_C - c_B)] \geq 0 \quad (3.49)$$

for the existence of these poles. When c_B and c_C are equal, Eq. (3.49) requires simply $\delta^2 \geq 8\mu_2^{(0)}$. In the BC binary-alloy limit Eq. (3.49) becomes $\delta^2 c_B c_C \geq \mu_2^{(0)}$ as expected from Eq. (3.47).

IV. NUMERICAL RESULTS FOR THE SEMIELLIPTIC BAND

In this section we discuss results for the semi-elliptic band.³² The presence of four independent

parameters in the general description of the ternary alloy—twice as many as in the binary case—admits a wide variety of numerical possibilities for illustrating the average Green's-function formalism of Secs. I–III. Some numerical applications were presented in I, and the aim of this section is to extend these considerations to new examples providing further insight into the nature of three-component systems in the CPA.

On making use of Hubbard's semielliptic model density of states for the band structure of the reference crystal, i.e.,

$$D_0(E) = \begin{cases} (\frac{1}{2}\pi)(1-E^2)^{1/2} & \text{if } |E| \leq 1, \\ 0 & \text{otherwise,} \end{cases} \quad (4.1)$$

the integration over E in Eq. (2.22) yields the relation

$$F(z) = F_0(z - \Sigma) = 2(z - \Sigma) - 2[(z - \Sigma)^2 - 1]^{1/2}. \quad (4.2)$$

We may combine Eq. (4.2) or its inverse, which expresses Σ in terms of F , together with Eq. (3.17) to obtain quartic equations for Σ and F . Once these quantities are known, the total density of states $D(E)$ and the spectral density $\rho(\vec{k}, z)$ are computed from Eqs. (2.23) and (3.6). The partial densities of states $D_{A,B,C}(E)$ are obtained from the formula

$$D_{A,B,C}(E) = -\pi^{-1} \times \text{Im} \left(\frac{F(z)}{1 - [\epsilon_{A,B,C} - \epsilon_A - \Sigma(z)]F(z)} \right)_{z=E+i0}. \quad (4.3)$$

The reader is referred to I for additional details concerning these functions and the quartic equations for Σ and F . Numerical results in this paper and those in I originate from the solutions of these equations yielding two real and two complex roots, the physical root being the one with negative-imaginary part. The case of four complex roots never occurs. As already mentioned, we deal with the setup in which the host level $\epsilon_A = 0$ is higher than the C impurity level, but lower than the B impurity level so that important effects of alloying will appear at the top and bottom of the reference band and beyond.

We begin our discussion by considering the self-energy plotted as a function of E . Figures 1(a)–1(f) illustrate the real part and the absolute magnitude of the imaginary part of $\Sigma(z)$ for fixed concentrations $c_B = c_C = 0.16$, and various values of β and λ . These representative values of the parameters yield the varieties of behavior expected in $\Sigma(z)$. We identify six regimes and give an example of each in Fig. 1. In these cases the an-

alytic structure of $\Sigma(z)$ is distinguished by a single cut along the real axis (unsplit band), two cuts (singly split band), two cuts separated by a pole, three cuts (doubly split band), three cuts with a pole between one adjacent pair, and finally three cuts with a pole between each adjacent pair. Figure 1(a) is an example of the alloy in the unsplit band situation. The special choice $\beta = -\lambda = 0.50$ causes $|\text{Im}\Sigma|$ (henceforth called \mathcal{I}) to be symmetric and $\text{Re}\Sigma$ (henceforth called \mathcal{R}) anti-symmetric in E . The humps in the former quantity near the top and bottom of the band denote a strong damping of the electron states at these energies due to scattering by impurities. These large values of \mathcal{I} are accompanied by rapid shifts in the spectrum due to precipitous changes in \mathcal{R} . The slower variation of Σ around the origin of energy is indicative of a virtual-crystal-type behavior where \mathcal{I} is relatively small compared with the peaks which appear on either side of the $E = 0$ region, and \mathcal{R} is nearly constant. Indeed, the closer β or λ approaches the origin, the more this behavior spreads over the upper or lower portions of the band. For all cases studied, the self-energy tends to its limiting value Δ_1 from above (below) in the positive (negative) energy asymptotic region. Figure 1(b) shows that an increase in β from 0.50 to 1.20, with the other parameters held fixed, produces the splitting off of a single impurity subband from the main band. The strongest damping takes place in the neighborhood of the gap edge of the subband where B -impurity scattering is most effective. The majority subband, especially over its middle region, has the virtual crystal character mentioned above. If at this point we continue to increase β with no change in the other parameters, it is found that \mathcal{I} in the impurity subband increases rapidly and maximizes as soon as the pole appears in the gap. Under these conditions there is no marked difference in the majority subband. Just as in VKE, we may interpret this situation in terms of the sum rules referred to in the paragraph following Eq. (3.44). Although the sum rule for the lower subband is strictly valid only for large (β) splitting and small $|\lambda|$, it is already satisfied in the CPA with $D_0(E)$ given by Eq. (4.1) at the moment the impurity subband exists. Consequently, as β increases, \mathcal{I} in the α subband remains essentially unchanged from that in Fig. 1(b). On the other hand, when the pole appears, the integral of \mathcal{I} over both subbands saturates at the value $-\pi\mu_2^{(0)}$, and as a result \mathcal{I} in the impurity subband behaves as noted above. In going from Fig. 1(b) to Fig. 1(c) we see an example where the split-off subband is separated from the majority subband by a pole in Σ at $E_0 = 2.5$. At the same time the more

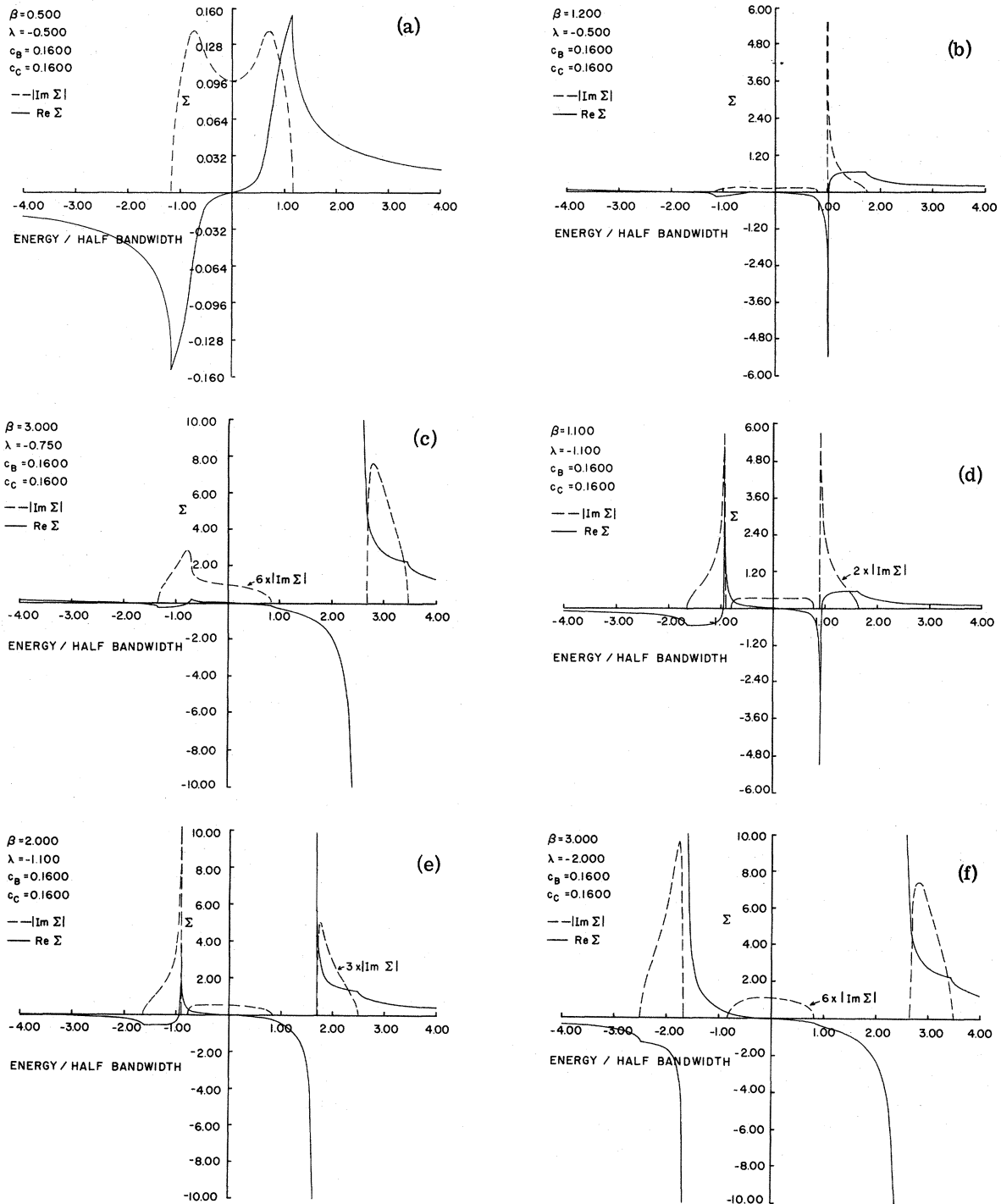


FIG. 1. Real part (solid line) and absolute value of the imaginary part (dashed line) of the self-energy Σ . These examples represent an unsplit band (a), a singly split band (b), singly split band with a pole in Σ at $E_0 = 2.5$ (c), doubly split band (d), doubly split band with a pole at $E = 1.65$ (e), and a doubly split band with poles at $E = 2.48$ and $E = -1.64$ (f).

negative value of $\lambda (= -0.75)$ gives rise, at the lower energies of the main band, to a prominent hump in \mathcal{R} which, of course, would not have occurred had λ remained constant as in the previous discussion. Again, an increase in β beyond the point at which the impurity subband first arises causes no marked difference in the lower subband, while \mathcal{R} in the upper subband, which in Fig. 1(c) is well into the pole region, behaves as before. Needless to say, it is no longer accurate, because of the large value of $|\lambda|$, to apply our λ -independent sum rule for the lower subband to the situation depicted in Fig. 1(c).

Three cases of the doubly-split-band regime are shown in Figs. 1(d)–1(f). In the first of these, $\beta = -\lambda = 1.10$, the splittings are symmetrical and no poles appear. The damping is now very pronounced in the neighborhood of the gap edge of the upper and lower impurity subbands where B -impurity and C -impurity scatterings are most effective, respectively. Figure 1(e), $\beta = 2.0$ and $\lambda = -1.10$, gives an example of unsymmetrical splittings, and the presence of a pole at $E = 1.65$ separating the upper impurity subband from the majority subband. Finally, in Fig. 1(f), $\beta = 3.0$ and $\lambda = -2.0$, we present numerical conditions for unsymmetrical splittings, and poles at $E = 2.48$ and $E = -1.64$ between adjacent subbands.³³ In all three cases the alloy exhibits strong virtual crystal character in the host subband. It is of interest to examine in detail the effects of alloying on \mathcal{R} . Because the three subbands are nearly independent in the two-pole situation of Fig. 1(f), we have the advantage in the ternary alloy problem of knowing the behavior of \mathcal{R} over a subband which is essentially attributable to a single atomic species and disconnected from the asymptotic requirement on Σ . Thus the middle subband in Fig. 1(f) causes \mathcal{R} to increase and decrease precipitously in the regions immediately to its left and right, respectively, while inside the subband it decreases slowly with increasing E . The singularities which appear between independent subbands are the extrema of this behavior. It is emphasized that this is the general form of \mathcal{R} in the absence of the asymptotic condition, which has the strongest control on \mathcal{R} . For instance, by referring to the lower subband in Fig. 1(f) we see that \mathcal{R} has the characteristic structure described above except that it experiences the asymptotic influence on the left. A similar situation exists for the upper subband. As an exercise in the use of these observations let us explain the effects on \mathcal{R} due to the “impurity” parts and the “host” part of the ternary alloy shown in Fig. 1(c). On the left-hand side of the lower subband, \mathcal{R} tends to its limiting value. Upon entering the bottom of this subband, it comes

under the influence of a weak concentration of “ C impurities” which, if acting as independent constituents with a center of influence at -0.75 , would tend to drive \mathcal{R} down, gently at first and then more steeply. Meanwhile, the heavier concentration of “host impurities” would, if also acting alone, at first force \mathcal{R} up. The effects of alloying in the subband are manifested in the conflict between the characteristics each impurity type would impose if acting this way. Instead of decreasing in the “ C -impurity” region \mathcal{R} increases slightly and then more rapidly as the “host impurity” takes over. This is followed by a predictable gradual decrease in \mathcal{R} across the “host-impurity” region. Beyond the upper edge of the lower subband \mathcal{R} behaves as expected.

To continue with our numerical presentation of the \bar{k} -independent properties of the averaged ternary alloy in the CPA, we now exhibit some “three-dimensional” plots of the total density of states $D(E)$, and the three partial densities of states $D_{A,B,C}(E)$. Having solved the quartic equations for $F(E)$ and $\Sigma(E)$, we obtain these quantities from Eqs. (2.23) and (4.3). These new calculations of $D(E)$ and $D_{A,B,C}(E)$ supplement those given in I where the effects of disorder are most pronounced at the top of the host band or above it. For economy of illustration we provide only one sequence of figures involving the singly and doubly split bands. Furthermore, the latter case is specialized to show the development of $D(E)$ only when the scattering strengths are equal and opposite. Figure 2 displays $D(E)$ for (a) $\beta = -\lambda = 0.50$, $c_C = 0.10$, (b) $\beta = 1.0$, $\lambda = -0.50$, $c_C = 0.10$, and (c) $\beta = -\lambda = 1.0$, $c_C = 0.05$. In Fig. 2(a) there is distortion of the band which is localized near the upper edge for small c_B and spreads over large portions of the band with increasing c_B . Upon increasing β to 1.0, as shown in Fig. 2(b), an impurity subband splits off the upper edge of the majority subband. Further increases in β , in this case, cause the impurity subband to shift to higher energies. Eventually, we are led to a stage comparable to Fig. 1(c) where the impurity subband becomes independent. This shows up most strikingly in the partial density of states for B atoms. For example, the case $\beta = 3.0$, $\lambda = -0.75$ and $c_C = 0.16$ of Fig. 5 shows that $D_B(E)$ makes no visible contribution to the majority subband density of states. A detailed numerical determination of the height and width of the impurity subband in Fig. 2(b) indicates that these quantities are proportional to $(c_B)^{1/2}$, or approximately so, in agreement with Eqs. (3.23) and (3.25). Analogously, the majority subband satisfies Eqs. (3.26) and (3.27) for small c_B . In the singly-split-band situation of Fig. 2(b), the impurity subband and the majority subband have, within numerical ac-

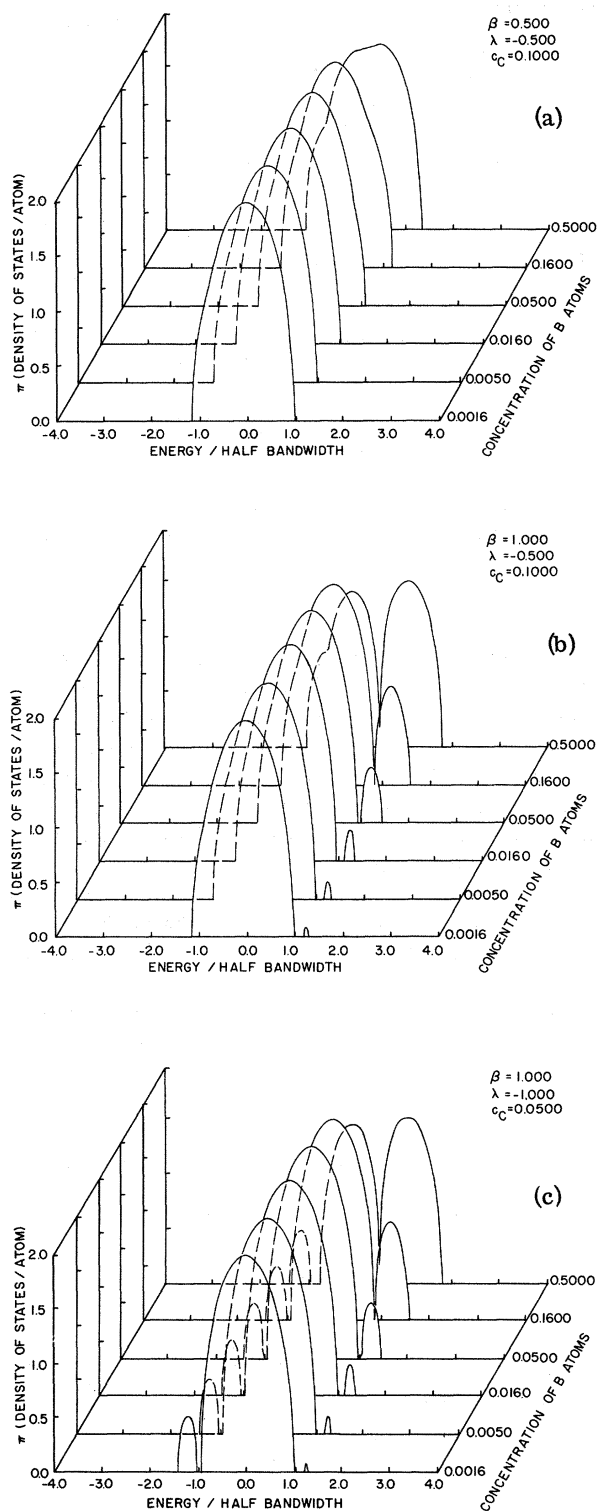


FIG. 2. Total density of states for various values of B atom concentration while the parameters β , λ , and c_C have the values (a) 0.50, -0.50, 0.10, (b) 1.0, -0.50, 0.10, and (c) 1.0, -1.0, 0.05, respectively. The energy origin coincides with the center of the pure A band.

curacy, integrated densities equal to c_B and $c_A + c_C$, respectively. Our final example of $D(E)$ is shown in Fig. 2(c). Comparison with the previous case shows that $|\lambda|$ and c_C have been increased and decreased to 1.0 and 0.05, respectively. The scattering strengths show, once again, their importance in forcing the "impurity" parts of the main band to split off. The main effects of running through the sequence in Fig. 2 with a still lower value of c_C —say, $c_C = 0.005$, are (i) to decrease the size of the lower impurity subband in Fig. 2(c), and (ii) the removal of the distortion at the lower edge of the main band in Figs. 2(a) and 2(b). Heights, widths, and integrated densities of the three subbands in the doubly-split-band regime vary with concentrations as before.

The contribution of a particular type of site (A, B, or C) to the total density of states can be studied through its partial or local-state density given by Eq. (4.3). We recall from I that the total density of states is the sum of the concentrated-weighted partial densities of states. For this purpose, we present three examples showing these quantities in (i) singly- and doubly-split-band situations, and (ii) a singly-split-band case with one pole in the self-energy. For clarity of display, the B component is exhibited separately in the first two examples. The total density of states in Fig. 2(b) is resolved into its components in Fig. 3. Because of the large value of β , the chief contributor to the impurity subband is $D_B(E)$ which has the form plotted in Fig. 3(b). For low concentrations of B atoms, $D_B(E)$ approximates the Koster-Slater³⁴ density of states due to a single impurity. The AC binary alloy and impurity characteristics of the majority subband in Fig. 2(b) are featured in Fig. 3(a). The $D(E)$ for the alloys of Fig. 2(c) is decomposed in Figs. 4(a) and 4(b). The outcome is quite predictable as these figures show. A further decrease in c_C would cause a narrowing and heightening of the vertical structure at the lower energies in $D_C(E)$. We demonstrate in Fig. 5, $\beta = 3.0$, $\lambda = -0.75$, $c_C = 0.16$, the independence of an impurity subband for large scattering strength, a situation of physical importance when one constituent is well separated from the other two. Another physically interesting possibility is the case of three such well-separated subbands.

To end this section, we now consider the spectral density $\rho(\vec{k}, E)$. This important \vec{k} -dependent quantity is related to the average Green's function $G(\vec{k}, z)$ by Eq. (3.5), and therefore possesses information concerning the single-particle spectrum of the model. In this connection, it is particularly useful for describing quasiparticle-type excitations, i.e., particlelike excitations having a well-defined or nearly-well-defined energy for a given

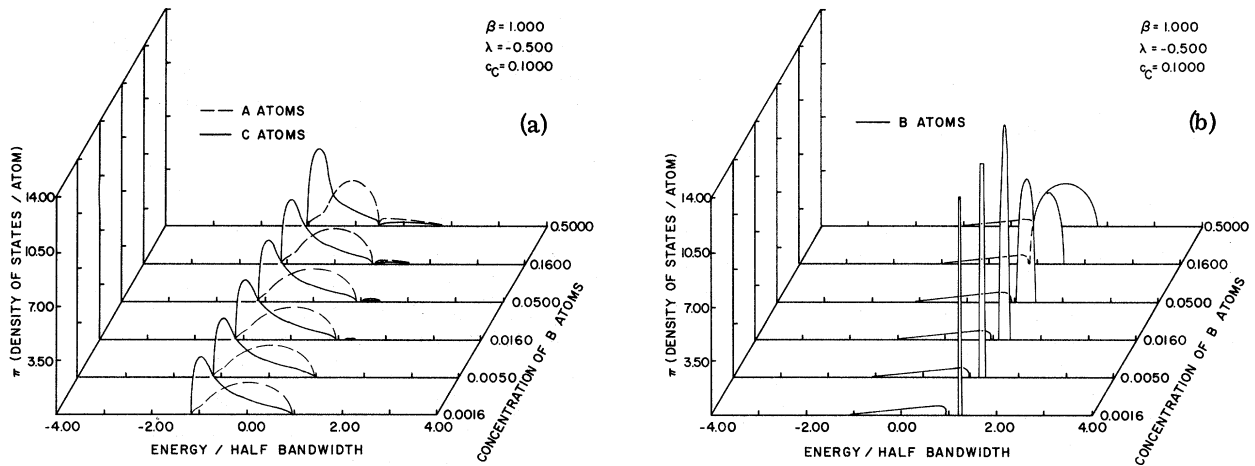


FIG. 3. Component densities of states as defined by Eq. (4.3) for the alloys of Fig. 2(b). (a) Illustrates D_A (dashed line) from the A (majority) sites and D_C (solid line) from the C (minority) sites. (b) Shows D_B from the B (minority) sites.

definite momentum. In the coherent potential approximation the self-energy is independent of wave vector, so the \vec{k} dependence in $G(\vec{k}, z)$ and $\rho(\vec{k}, E)$ is due entirely to the structure factor $S(\vec{k})$ introduced in Eq. (2.3). Further insight into the significance of $\rho(\vec{k}, E)$ is obtained from its δ -function form $\delta(E - S(\vec{k}))$ which results when $\Sigma(E)$ is zero and there is no substitutional disorder in the system. This follows from Eqs. (2.21) and (3.4). In that case $\rho(\vec{k}, E)$ gives rise to undamped \vec{k} states, and its half-width is zero. The spectral density for various values of $S(\vec{k})$ ranging from -1 to $+1$ are shown in Fig. 6. From the first example, $\beta = 3.0$, $\lambda = -2.0$, $c_B = c_C = 0.16$, given in Fig. 6(a),

we see that $\rho(\vec{k}, E)$ contains three well-separated peaks for each value of \vec{k} represented through $S(\vec{k})$. The approximately Lorentzian shape of the middle peak, except at the band edge, is characteristic of a quasiparticle state with wave vector \vec{k} and a mean lifetime which is inversely proportional to the half-width of the spectral density. An increase in $S(\vec{k})$ causes its position to shift to a higher energy. This type of excitation is associated with the plane-wave-like eigenstates of the perfect A-atom crystal. On the other hand, the lower and upper peaks of $\rho(\vec{k}, E)$ are nonquasiparticlelike over the entire band and do not shift with $S(\vec{k})$. The shapes of these components are characteristic of

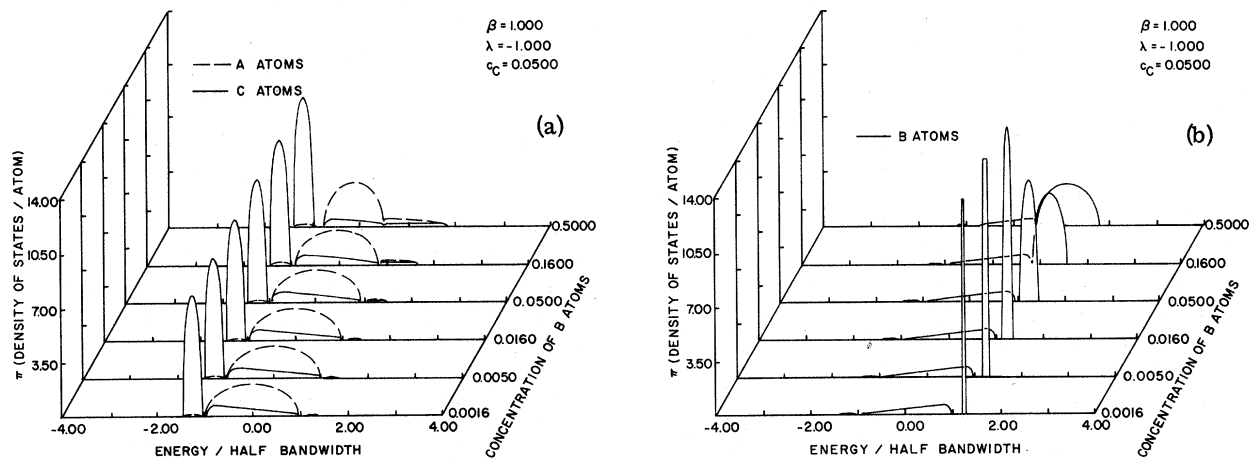


FIG. 4. Component densities of states as defined by Eq. (4.3) for the alloys of Fig. 2(c). (a) Shows D_A (dashed line) from the A (majority) sites and D_C (solid line) from the C (minority) sites. (b) Gives D_B from the B (minority) sites.

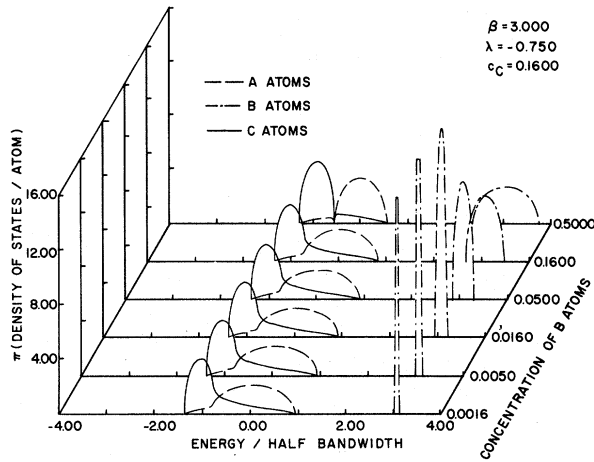


FIG. 5. Component densities of states as defined by Eq. (4.3) for the case $\beta = 3.0$, $\lambda = -0.75$, and $c_C = 0.16$. Note that the $c_B = 0.16$ curve corresponds to Figs. 1(c) and 6(b). This example illustrates D_A (dashed line) from the A (majority) sites, D_C (solid line) from the C (minority) sites, and D_B (dashed-dotted line) from the B (minority) sites for the situation where the band is singly split with one pole in the self-energy.

excitations which are localized in coordinate space, and as indicated by Fig. 1(f), are related to the highly damped impurity states which have split off from the main subband. In Fig. 6(b), where $\beta = 3.0$, $\lambda = -0.75$ and the concentrations are the same as before, only one impurity subband has split off. The nature of the corresponding $\Sigma(E)$ is shown in Fig. 1(c). The majority subband has the properties of an unsplit binary alloy with quasiparticle behavior near the top of the band that is highly disturbed near $S(\vec{k}) = -1$. Similarly, in Fig. 6(c), $\beta = -\lambda = 0.75$, where the band is no longer split, the quasiparticle structure is also strongly effected in the vicinity of $S(\vec{k}) = +1$. In these figures, as opposed to Fig. 6(a), there is a greater localization in \vec{k} space of the states controlled by the impurity parameters ϵ_C and ϵ_C and ϵ_B , respectively. This means, of course, that the corresponding states in coordinate space are less localized, and similarly to VKE this behavior is predictable when ϵ_C and/or ϵ_B approach ϵ_A .

At this point we wish to comment briefly on the problem of correlating the qualitative quasiparticle behavior of $\rho(\vec{k}, z)$, seen in the above numerical considerations, with the appearance of poles in the continuation of $G(\vec{k}, z)$ into the lower-half z plane. These poles are found by solving the cubic equation for z that results when $z - \Sigma = S(\vec{k})$ is used to eliminate Σ from Eq. (3.17). Without presenting a detailed examination of this equation, we generalize from the results of VKE, for weak couplings

and/or small concentrations, that (i) one of its roots will have a straightforward connection with the Lorentzian structure in $\rho(\vec{k}, z)$, (ii) the other two roots will have no such identifiable relation-

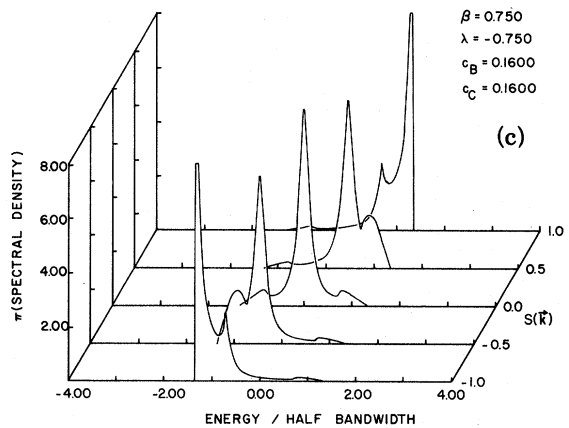
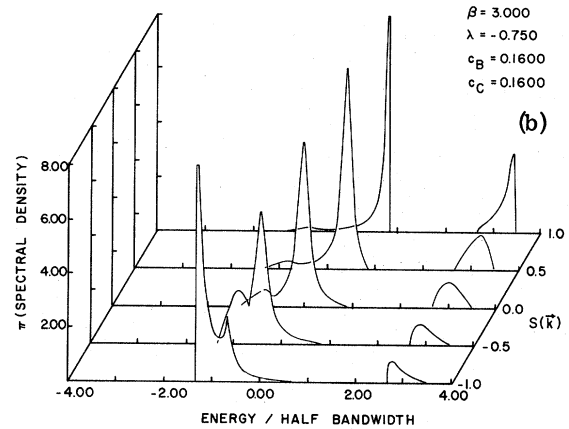
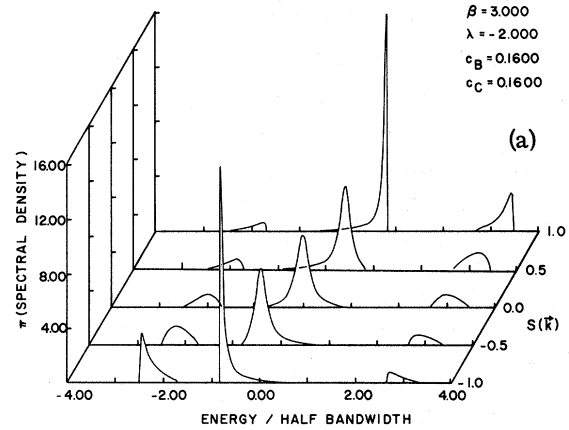


FIG. 6. Spectral density $\rho(\vec{k}, E)$ as a function of E at several values of $S(\vec{k})$ for (a) the three well-separated bands indicated by Fig. 1(f), (b) the singly-split-band case of Fig. 1(c), and (c) an unsplit-band situation, $\beta = -\lambda = 0.75$, $c_B = c_C = 0.16$.

ship, and (iii) the non-Lorentzian impurity regions of the spectrum do not associate with poles. Furthermore, for strong couplings and/or large concentrations, we may expect no clear interpretation of all three poles. From the viewpoint of VKE this could indicate a failure of the quasiparticle interpretation for strong couplings, or a shortcoming of the CPA. This problem remains unresolved.

V. CONCLUDING REMARKS

The aim of the present series of papers is to develop a fundamental understanding of disordered ternary alloys comparable to that already achieved for the binary type. For initial purposes, we approach the problem through the study of an elementary model which does not purport to represent any particular substance, but which may possess some features appearing in real systems. The usual single-band model and its various modifications have acquired much importance as a general testing ground for the CPA and other promising ideas in alloy theory. Within the framework of this model we have extended the CPA calculation to ternary compounds. The alloy Hamiltonian in the binary case is specified in terms of two parameters, while in the ternary case, four are required. These additional degrees of freedom make the study of three-component systems more complicated, and correspondingly puts a higher requirement on the capability of the CPA. Numerical results show that this approximation provides a reasonable description of simple ternary alloys over a wide range of concentrations and scattering strengths.

The calculations of this paper and I provide a point of departure for many possibilities concerning a more realistic treatment of the ternary problem. As already mentioned, it seems worthwhile to take into account the alloying of constituents

with different bandwidths. One way of doing this is by allowing for various amounts of randomness in the six interatomic transfer integrals $A-A$, $B-B$, $C-C$, $A-B$, $A-C$, and $B-C$. In this connection, we can also think of introducing a system of muffin-tin potentials as previously considered by Soven¹¹ in the binary case. Another concern is the study of cluster effects. A preliminary report of the ternary-pair calculation is given in Ref. 35. At this point it appears that convergence difficulties in these results can be avoided as in the binary case¹⁷ by including off-diagonal randomness. This problem is presently under investigation. Finally, it remains to comment on applying the CPA to some actual three-component physical systems such as the alloys of copper, nickel, and zinc. The binary alloys of these metals have been studied extensively by a variety of theoretical and experimental approaches, and it would be appropriate to investigate the electronic structure of the corresponding ternary compounds. Of course, the complicated band structure of these metals precludes the direct application of the present model based on a nondegenerate tight-binding band. A Hamiltonian of the type proposed by KVE, but generalized to three constituents, seems like a physically reasonable starting point. Following the methods of Ref. 20, it should then be possible to treat Cu-Ni-Zn alloys of arbitrary concentrations. On the other hand, an equally challenging extension would be to try the ATA method of Ref. 29 on this ternary system.

ACKNOWLEDGMENTS

The authors are grateful to the University of Vermont Academic Computing Center and the director, T. Thomas, for making its resources available under its research support program. Thanks are also due to J. S. Brown for his critical reading of the manuscript.

*Work supported by the U. S. Atomic Energy Commission under Contract No. AT(11-1)3551, the International Business Machines Corporation, and in part by Grant No. GU-3774-158 of the National Science Foundation.

†Work supported by Grant No. GU-3774-158 of the National Science Foundation.

¹P. Soven, Phys. Rev. **156**, 809 (1967); D. W. Taylor, *ibid.* **156**, 1017 (1967); Y. Onodera and Y. Toyozawa, J. Phys. Soc. Jpn. **24**, 341 (1968). An extensive list of references to the CPA and its applications is given in the review article by F. Yonezawa and K. Morigaki, Prog. Theor. Phys. Suppl. **53** (1973).

²M. Lax, Rev. Mod. Phys. **23**, 287 (1951).

³B. Velický, S. Kirkpatrick, and H. Ehrenreich, Phys.

Rev. **175**, 747 (1968).

⁴P. W. Anderson, Phys. Rev. **109**, 1492 (1958). The Anderson model is essentially the same as the Hamiltonian of Eqs. (2.1) and (2.2) except that instead of the site energy ϵ_n having two (three) possible values as in the binary (ternary) alloy, it possesses a distribution density $P(\epsilon_n)$ with a width centered around a mean value.

⁵J. Hubbard, Proc. R. Soc. Lond. A **281**, 401 (1964).

⁶E. A. Stern, Phys. Rev. Lett. **25**, 1630 (1971); Phys. Rev. B **9**, 1170 (1974).

⁷J. A. Blackman, N. F. Berk, and D. M. Esterling, Phys. Rev. B **4**, 2412 (1971); H. Shiba, Prog. Theor. Phys. **46**, 77 (1971).

⁸T. Matsubara and T. Kaneyoshi, Prog. Theor. Phys. **36**,

- 695 (1966). A summary of the locator method is given by J. M. Ziman, *J. Phys. C* **2**, 1230 (1969).
- ⁹F. Brouers, *Solid State Commun.* **10**, 757 (1972); F. Brouers and J. van der Rest, *J. Phys. F* **2**, 1070 (1972).
- ¹⁰J. A. Blackman, *J. Phys. F* **3**, L31 (1973); L. Schwartz, H. Krakauer, and H. Fukuyawa, *Phys. Rev. Lett.* **30**, 746 (1973); F. Brouers, F. Ducastelle, and J. van der Rest, *J. Phys. F* **3**, 1704 (1973); R. Bass and P. L. Leath, *Phys. Rev. B* **9**, 2769 (1974).
- ¹¹P. Soven, *Phys. Rev. B* **2**, 4715 (1970); B. L. Gyorffy, *ibid.* **5**, 2382 (1972).
- ¹²T. Kaplan and M. Mostoller, report, 1973 (unpublished).
- ¹³E.-N. Foo and D.-H. Wu, *Phys. Rev. B* **5**, 98 (1972); R. Harris, M. Plischke, and M. J. Zuckermann, *Phys. Status Solidi B* **53**, 269 (1972); J. B. Parkinson, *J. Phys. C* **6**, 2337 (1973).
- ¹⁴H. Matsuda, *Prog. Theor. Phys.* **27**, 811 (1962); J. Hori, *ibid.* **32**, 471 (1964); R. E. Borland, *Proc. R. Soc. Lond.* **83**, 1027 (1964); J. Hori and M. Fukushima, *J. Phys. Soc. Jpn.* **19**, 296 (1964). For phonons, numerical calculations in one, two, and three dimensions reveal a peaky structure in the frequency spectrum generally understood to arise from clusters of light atoms. See review article by P. Dean, *Rev. Mod. Phys.* **44**, 127 (1972).
- ¹⁵R. N. Aiyer, R. J. Elliott, J. A. Krumhansl, and P. L. Leath, *Phys. Rev.* **181**, 1006 (1969); K. F. Freed and M. H. Cohen, *Phys. Rev. B* **3**, 3400 (1971); F. Cyrot-Lackmann and F. Ducastelle, *Phys. Rev. Lett.* **27**, 429 (1971); B. G. Nickel and J. A. Krumhansl, *Phys. Rev. B* **4**, 4354 (1971); M. Nakamura and F. Yonezawa, *Prog. Theor. Phys.* **47**, 1124 (1972); V. Capek, *Phys. Status Solidi*, **43**, 61 (1971); L. Schwartz and E. Siggia, *Phys. Rev. B* **5**, 383 (1972); P. L. Leath, *ibid.* **5**, 1643 (1972); L. Schwartz and H. Ehrenreich, *ibid.* **6**, 2923 (1972); J. Mertsching, *Phys. Status Solidi* **59**, 227 (1973); E.-N. Foo and S. M. Bose, report (unpublished); H. J. Fischbeck, *Phys. Status Solidi B* **62**, 425 (1974).
- ¹⁶F. Ducastelle, *J. Phys. C* **4**, L75 (1971); B. G. Nickel and W. H. Butler, *Phys. Rev. Lett.* **30**, 373 (1973); P. L. Leath, *J. Phys. C* **6**, 1559 (1973).
- ¹⁷E.-N. Foo, H. Amar, and M. Ausloos, *Phys. Rev. B* **4**, 3350 (1971); F. Cyrot-Lackmann and M. Cyrot, *J. Phys. C* **5**, L209 (1972); T. Morita and C. C. Chen, *J. Phys. Soc. Jpn.* **34**, 1136 (1973); A. Bergmann and V. Halpern, *J. Phys. C* **7**, 289 (1974); K. Moorjani, T. Tanaka, M. M. Sokoloski, and S. M. Bose, *ibid.* **7**, 1098 (1974).
- ¹⁸We refer only to a select few of these. For further examples see review article mentioned in Ref. 1.
- ¹⁹S. Kirkpatrick, B. Velický, and H. Ehrenreich, *Phys. Rev. B* **1**, 3250 (1970), abbreviated as KVE.
- ²⁰G. M. Stocks, R. W. Williams, and J. S. Faulkner, *Phys. Rev. Lett.* **27**, 253 (1971); *Phys. Rev. B* **4**, 4390 (1971).
- ²¹G. M. Stocks, R. W. Williams, and J. S. Faulkner, *J. Phys. F* **3**, 1688 (1973).
- ²²S. Hüfner, G. K. Wertheim, and J. H. Wernick, *Phys. Rev. B* **8**, 4511 (1973).
- ²³P. O. Nilsson, *Phys. Kondens Mater.* **11**, 1 (1970).
- ²⁴L. M. Scarfone, *Phys. Rev. B* **7**, 4435 (1973); **11**, 5211(E) (1975). We note that the present paper does not adhere completely to the notation used in I. See Ref. 31.
- ²⁵P. L. Leath, *Phys. Rev.* **171**, 725 (1968).
- ²⁶F. Yonezawa, *Phys. Rev. B* **7**, 5170 (1973).
- ²⁷T. Jo, H. Hasegawa, and J. Kanamori, *J. Phys. Soc. Jpn.* **35**, 57 (1973).
- ²⁸J. L. Beeby and S. F. Edwards, *Proc. R. Soc. Lond.* **A 274**, 395 (1962); J. L. Beeby, *ibid.* **279**, 82 (1964); J. L. Beeby, *Phys. Rev.* **135**, A 130 (1964); P. Soven, *ibid.* **151**, 539 (1966); L. Schwartz, F. Brouers, A. V. Vedyayev, and H. Ehrenreich, *Phys. Rev. B* **4**, 3383 (1971); A.-B. Chen, *ibid.* **7**, 2230 (1973); F. Ducastelle, *J. Phys. C* **7**, 1795 (1974).
- ²⁹A. Bansil, H. Ehrenreich, L. Schwartz, and R. E. Watson, *Phys. Rev. B* **9**, 445 (1974).
- ³⁰D. S. Saxon and R. A. Hutner, *Philips Res. Rep.* **4**, 81 (1949). See also J. Hori, *Spectral Properties of Disordered Chains and Lattices* (Pergamon, New York, 1968), and Appendix B of KVE.
- ³¹To agree with conventional notation, we let $F(E)$ and $F_0(E)$ replace $Z(E)$ and $Z_0(E)$ of I. In the present paper Z denotes the coordination number.
- ³²The figures included in this paper were the result of calculations performed on a Xerox Sigma 6 computer operating under the UTS and CP-V time-share monitors. The plots themselves were output on a Xerox Model 7531 Graph Plotter.
- ³³The energy values at which the poles are found in Figs. 1(e) and 1(f) are in agreement with those given by the square-root solutions of the quadratic equation for z that arises when the denominator in Eq. (3.43) is set equal to zero. For the special case of symmetrical double-band splitting, the poles are found at E_{\pm} , as numerical examples not included in this paper have verified.
- ³⁴G. F. Koster and J. C. Slater, *Phys. Rev.* **96**, 1208 (1954). The expressions for $D_{A,B,C}(E)$ in the dilute-alloy limit are given in I, Eq. (47).
- ³⁵R. L. Mauro and L. M. Scarfone, *Phys. Lett. A* **46**, 129 (1973).